

A critical review of unrealistic results in SCAPS-1D simulations: Causes, practical solutions and roadmap ahead

Abhisek Saidarsan^{a,*}, Satyabrata Guruprasad^b, Ashish Malik^b, Pilik Basumatary^b, Dhriti Sundar Ghosh^{b,**}

^a Indian Institute of Science Education and Research, Pune, India

^b Thin-film and Photovoltaics Laboratory, Department of Physics, Indian Institute of Technology Dharwad, Dharwad, India



ARTICLE INFO

Keywords:

SCAPS-1D
Perovskite solar cells
Photovoltaics
Numerical simulation accuracy
Photovoltaic modelling discrepancies
Radiative recombination
Shockley-Queisser limit

ABSTRACT

One-dimensional Solar Cell Capacitance Simulator (SCAPS-1D) has become a widely used and popular electrical simulation tool in the photovoltaic community. Recently, with the realization of broad chemical tunability provided by perovskite materials, there has been a concerning increase in scientific papers reporting inflated solar cell device performance that deviates significantly from the best experimental results, with some even surpassing the fundamental Shockley-Queisser limit. While some of these projections might suggest significant potential for experimental advancements, it is crucial to approach such exaggerated results with caution. In this study, a comprehensive survey of over 250 reported perovskite solar cell architectures yielded the undeniable implication that such results are primarily due to unrealistic input parameters such as low radiative recombination coefficient, low defect densities, and high doping concentrations. Additionally, inconsistencies in simulation methods and the optical limitations of SCAPS-1D have also been explored. To address these issues, several recommendations, including a standard simulation protocol, have been proposed. Software-generated results may not always represent the actual cell performance as they heavily rely on the validity of inputs and software algorithms.

1. Introduction

The availability of energy has revolutionised humankind over the past few centuries. However, the ever-increasing demand for energy and the detrimental environmental impact of using fossil fuels has accelerated the quest to search for alternative, cleaner and sustainable sources of energy. Among renewable energy resources, solar energy is unparalleled in its potential. The total solar energy reaching the earth in 1 h is more than enough to meet the annual energy demand of the entire globe [1].

As a result, the field of photovoltaics (PV) has gained a lot of traction in the research community in recent times. The efficiency of solar cells has increased significantly over the past decade. In practice, while crystalline silicon solar cells have achieved a confirmed sub-module efficiency (CSME) of $26.8 \pm 0.4\%$, GaAs thin-film cells have achieved a remarkable efficiency of $29.1 \pm 0.6\%$ by 2023 [2]. Although a relatively newer technology, perovskite solar cells (PvSCs) have rapidly

progressed since their introduction to the PV field in 2009 to boast an efficiency of $26.1 \pm 0.8\%$ by 2023 [2].

Modelling and simulation are essential parts of the scientific and engineering process when it comes to the experimental realization of efficient and economical solar cells. They provide a number of benefits before physical experiments are conducted, such as saving time, system understanding and prediction, and optimization. Solar-cell Capacitance Simulator (SCAPS)-1D is an extensively used one-dimensional solar cell simulation tool developed at the University of Gent, Belgium, to simulate and maximize the performance of solar cell devices (please refer to SI for more details) [3,4]. Although it was originally developed for cell structures of CuInSe₂ and CdTe family, it has advanced over the years to simulate virtually any solar cell, making it an indispensable tool in the field of solar photovoltaics research. It can simulate the electrical characteristics of solar cells, including current-voltage (I-V), capacitance-voltage (C-V), capacitance-frequency (C-f) and Quantum efficiency profiles, which are essential in optimising the performance of

* Corresponding author.

** Corresponding author.

E-mail addresses: abhisek.saidarsan@students.iiserpune.ac.in (A. Saidarsan), dhriti.ghosh@iitdh.ac.in (D.S. Ghosh).

a solar cell. Through its comprehensive electrical modelling capabilities, it has enabled researchers to identify optimal device architectures and configurations by providing valuable insights into the performance of a myriad of different possible combinations of materials for PV cells. Over the years, it has incorporated several advanced features, including defect modelling, interface recombination, gradable parameters, tunnelling effects, and temperature variations, all within a user-friendly graphical user interface, which has improved its simulation accuracy and broadened its applicability. Since its introduction to the research community, SCAPS-1D has not only deepened the theoretical understanding of various photovoltaic mechanisms but has also played a pivotal role in guiding experimental design and fabrication [3,4].

The material perovskites refer to a broad class of molecules with a crystal structure similar to the mineral perovskite, CaTiO_3 . Perovskite materials for solar cell applications were first reported in 2009 [5]. Since then, they have rapidly emerged as one of the most promising photovoltaic technologies. Apart from two electrodes with one of them transparent, a conventional PvSC consists of an absorber layer (perovskite) sandwiched between two charge transport layers- Electron Transport Layer (ETL) and Hole Transport Layer (HTL), which ensure proper separation and transport of the photogenerated carriers. Superior optoelectronic properties of perovskite materials such as bandgap tunability, strong absorption in the visible region, bipolar carrier transport ability, high charge carrier mobility, high carrier lifetime, low charge recombination rate and higher defect tolerance make them one of the preferred materials for PV applications. Additionally, low-cost processing techniques and ease of fabrication compared to other PV technologies have further accelerated the research in this field [6,7]. One of the most remarkable features of perovskite is that its crystal structure is capable of supporting a wide range of chemical entities (either atoms or atomic groups) that meet size and charge balances [6,7]. This property has allowed researchers to choose a wide range of absorber materials and charge transport layers, offering unprecedented flexibility in solar cell design. The possibility of enormously many combinations of materials has resulted in an exponential increase in the number of publications reporting SCAPS-1D simulations on perovskite solar cell architectures from 2009 onwards (Fig. 1). In recent times, via electrical simulations using SCAPS-1D, efficiencies of even up to 39 % have been reported in the scientific literature [8–10].

In a seminal paper in 1961, Shockley and Queisser (SQ) proposed a fundamental upper limit to the efficiency of solar cells. They assumed a single junction solar cell in which all photons incident with energy above the bandgap energy (E_g) generate precisely one electron-hole pair

(an exciton). The electron-hole pair undergoes thermal relaxation to lose energy in excess of the bandgap energy. They considered that radiative recombination is the only operating recombination mechanism and argued that even for an ideal solar cell, there exists a lower limit to the rate of radiative recombination. This determines the upper limit for the minority carrier lifetime, which leads to a fundamental upper bound to the performance achievable by any solar cell device [11]. For AM1.5G illumination, with no mechanisms of light concentration, the maximum SQ efficiency that a single junction solar cell can achieve is ~33.7 %, for an absorber with a bandgap energy of 1.34 eV [12]. However, the theory is only valid in the framework in which it is designed. In practice, several solar cell devices have been shown to exceed the SQ limit [13–16]. This can be attributed to the violation of one or more of the assumptions of the SQ limit framework. Several mechanisms such as multiple exciton generation, hot carrier solar cells, photon up-conversion, light concentration, intermediate band photovoltaics, lattice battery cells, fluorescent downshifting and photoferroics have been proposed in the scientific literature as potential pathways to exceed the SQ limit [14,17–19]. Since SCAPS-1D does not account for any of these mechanisms, the simulation results are expected to be confined within the theoretical SQ limit.

In this study, we conducted an extensive survey of over 250 PvSC architectures reported since 2020, which were published in ~180 research papers employing SCAPS-1D. Concerningly, it was found that an alarmingly high number of these publications claimed power conversion efficiencies (PCEs) that markedly exceeded the best experimental results, with some even surpassing the theoretical SQ limit (~33.7 %), as illustrated in Fig. 2. Despite the optimism that these projections inspire significant potential for experimental advancements, the validity of these results must be taken with profound scepticism, acknowledging the complexities and potential discrepancies between theoretical results and practical implementations. Accurate reporting of solar cell efficiency is paramount to the advancement of solar technology and the credibility of scientific research. However, the relentless pursuit of record efficiencies can be disastrous and counterproductive in the absence of an incentive to carefully and reliably simulate the performance of PV cells. It can mislead the scientific community, hinder progress, and undermine trust in the field. Although these practices do not suggest fraudulent intent, it was found that they arose from a lack of thorough understanding of the SCAPS-1D manual, convenience and some oversight in verifying the input parameters for the device. This lack of diligence may stem from very little motivation for the researcher to go the extra mile to ensure that correct input parameters are given,

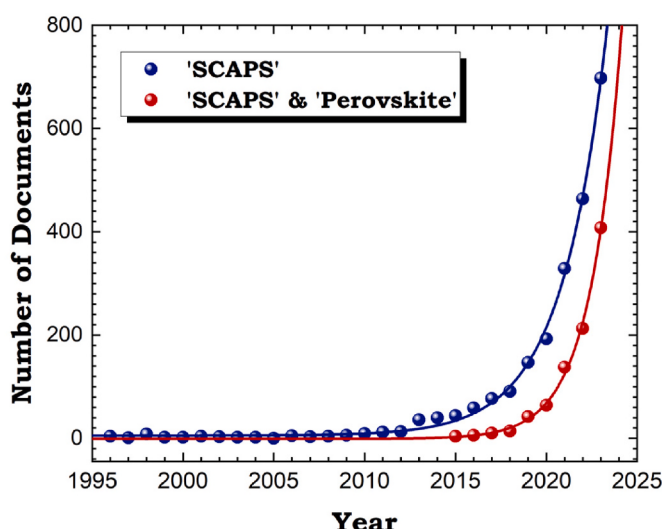


Fig. 1. Number of documents indexed on Scopus with 'SCAPS' and 'SCAPS' & 'Perovskite' in the fields- Article title, Abstract, or Keywords from 1996 to 2023.

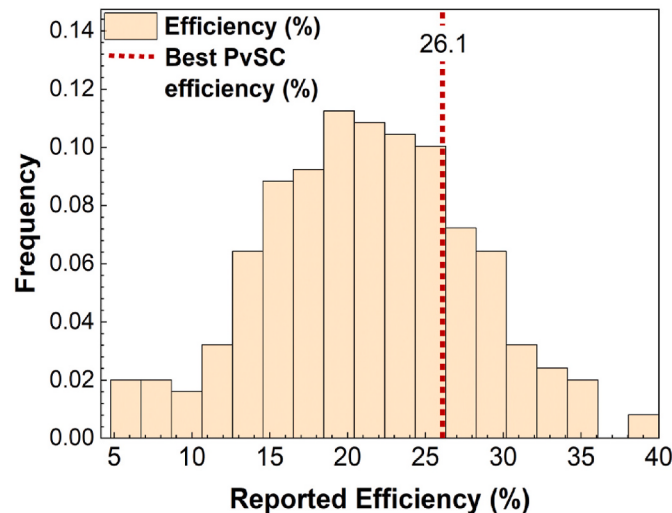


Fig. 2. Efficiencies reported in papers reporting simulations of single absorber layer PvSCs using SCAPS-1D. The dotted red line represents the best efficiency achieved by PvSCs by 2023 [2].

consistent with the laws of physics, especially if it could potentially result in lower performance, which can impede publication and funding. This inadvertently prioritises flashy and sensational results over methodological rigour.

One of the primary objectives of this study is to investigate the underlying factors contributing towards the overestimation of performance parameters of solar cells reported via electrical simulations using SCAPS-1D. Several potential reasons, including the accuracy and validity of input parameters, the lack of methodological rigour and the inherent optical limitations of SCAPS-1D, have been explored and critically examined. For instance, the use of simplified models and inaccurate assumptions about the device, such as employing idealised absorption models and neglecting recombination mechanisms and parasitic resistances, may lead to exaggerated and erroneous results. A critical analysis of how these simplifications impact simulation outcomes has been presented in this study. **A key challenge faced by users while performing simulations is to find accurate, material-specific input parameters from the literature.** Reliable experimental data for these attributes, especially for emerging PV materials like perovskites, are often scarce and are subject to wide variability depending on the fabrication methods used. We have demonstrated in this study that the use of attribute values that are not valid in the operational conditions of the solar cell would inevitably lead to obtaining unrealistic performance projections. This highlights the importance of ensuring that simulations are performed using data specific to a given fabrication process, and comparing them only with the corresponding experimental results. In this study, the necessity of using valid input parameters and the implementation of rigorous simulation methodologies has been emphasised. While SCAPS-1D is a very powerful tool for the simulation of photovoltaic devices, it is imperative to realise that software-generated results may not always represent the actual performance of the cell as they are highly dependent on the realism of the input parameters and the algorithms and approximations employed by the software. This study investigates these challenges and proposes several recommendations to ensure that the simulations yield more accurate and reliable results reflecting the true potential of the PV cell.

2. Methodology

For the survey, the keywords- ‘SCAPS’ & ‘Perovskite’ were searched for in several reputed journals, and the reported values of open circuit voltage (V_{oc}), short circuit current density (J_{sc}), Fill Factor (FF) and efficiency (η) were systematically compiled. These metrics were compared with the best experimentally obtained and, wherever available, externally verified performance data for the absorber material from the Perovskite Database Project (PDP) [20]. Furthermore, the reported simulation results were compared to the respective SQ limits calculated for AM1.5G illumination from Ref. [12]. A detailed assessment was conducted on MAPbI₃ and MASnI₃-based publications to identify potential discrepancies and inaccuracies in the simulation methods, as they were the most frequently used materials for the active layer among the surveyed papers. The most commonly used HTL and ETL for MAPbI₃ and MASnI₃-based devices were Spiro-OMeTAD and TiO₂, respectively, due to their superior charge separation and transport abilities. Hence, similar analyses were performed on them. The analyses included examining trends and variability in the input parameters, as well as the methodologies used for optimising the performance of the device. In addition to material-specific analyses, the impact of using unrealistic parameters and optical limitations of SCAPS-1D on the device performance was investigated. This was done by simulating a device based on the architecture discussed in the paper referenced as [21], with the input parameters mentioned therein, as described in Table S1 in the Supporting Information (SI) and using the default AM1.5G spectrum available in SCAPS-1D (Version 3.3.11).

3. Detailed survey outcome and discussions

In the context of the survey carried out in this work, it has been found that a diverse array of solar cell architectures has been reported. Several perovskites, including MAPbI₃, MASnI₃, CsSnCl₃ and CsSnI₃, emerged as popular materials for absorber layers. Historically MAPbI₃ was among the first perovskites to be demonstrated for solar cell applications [5] and has been extensively studied since its introduction. Later, lead-free MASnI₃ became a popular choice owing to the toxicity concerns associated with lead-based perovskites. These materials have been widely studied as absorber materials in the PV community due to the proximity of their bandgaps to the ideal SQ bandgap of 1.34 eV [12]. However, the presence of the organic cation CH₃NH₃⁺ in the A site of these ABX₃ perovskites has resulted in higher thermal instability. For instance, at temperatures around 85 °C, MAPbI₃ (CH₃NH₃PbI₃) decomposes into PbI₂ and other products. On the other hand, CsPbI₃ exhibits better thermal tolerance, decomposing only at temperatures as high as 450 °C [22]. This led to the rise in popularity of all-inorganic perovskites such as CsPbX₃ and CsSnX₃, where X represents a halide ion (I⁻, Br⁻, Cl⁻). Among the charge transport layers, Spiro-OMeTAD, PEDOT:PSS and copper-based inorganic materials like Cu₂O and CuI were commonly used as hole transport layers (HTL), while TiO₂, PCBM, and ZnO and were found to be popular choices for electron transport layers (ETL) for the surveyed MAPbI₃ and MASnI₃-based devices. These materials were selected owing to their superior charge separation and transport capabilities, which result in enhanced power conversion efficiency. Additionally, lower charge recombination rates, enhanced stability and ease of processing and fabrication of these materials have further contributed to their popularity [6,23,24].

Despite the progress in perovskite photovoltaics simulation, the literature survey revealed a concerning trend of numerous publications reporting inflated device performance metrics, which can mislead the scientific community about the true potential of PvSCs. Notably, nearly 25 % of the surveyed MAPbI₃-based PvSCs claimed PCEs that exceeded their best experimental efficiency by more than 20 %. This figure was even higher for MASnI₃-based PvSCs, with more than 90 % of publications reporting similarly exaggerated efficiencies (Fig. 3(a) and (b)). The short circuit current density (J_{sc}) exhibited similar overestimations for 15.4 % and 80.6 % of MAPbI₃ and MASnI₃-based stacks respectively, while for open circuit voltage, the figures were 12.8 % and 35.5 %, respectively. Although the dataset was relatively small, it clearly indicates a troubling prevalence of a high frequency of inflated results obtained via electrical modelling using SCAPS-1D.

Alarmingly, numerous papers have claimed values that even exceed the SQ limit. Among the ~250 PvSC architectures surveyed, nearly 25 % of the reported V_{oc} and more than 10 % of the J_{sc} values surpassed this theoretical maximum (Fig. 4). Additionally, several papers reported values perilously close to the respective theoretical maxima, as depicted in Fig. 5. An overview of the survey findings has been presented in Table 1 for ease of comparison and context. This highlights a disturbing extent of overestimation of device performance using SCAPS-1D, emphasizing the need for a standardized and rigorously enforced simulation protocol.

A comprehensive analysis of the surveyed papers indicates that the inflated simulation results for device performance using SCAPS-1D arise from several inconsistencies and oversights in the simulation methodologies. This section presents a thorough overview of these findings and the factors contributing to inflated or unrealistic outcomes.

3.1. Attribute discrepancies and variability

Bandgap (E_g), dielectric permittivity(ϵ_r) and electron affinity(χ) are fundamental and intrinsic attributes of any material, primarily determined by temperature, lattice structure, electronic structure, doping density and chemical composition [25]. However, our survey uncovered several discrepancies and wide variability in the reported values of even

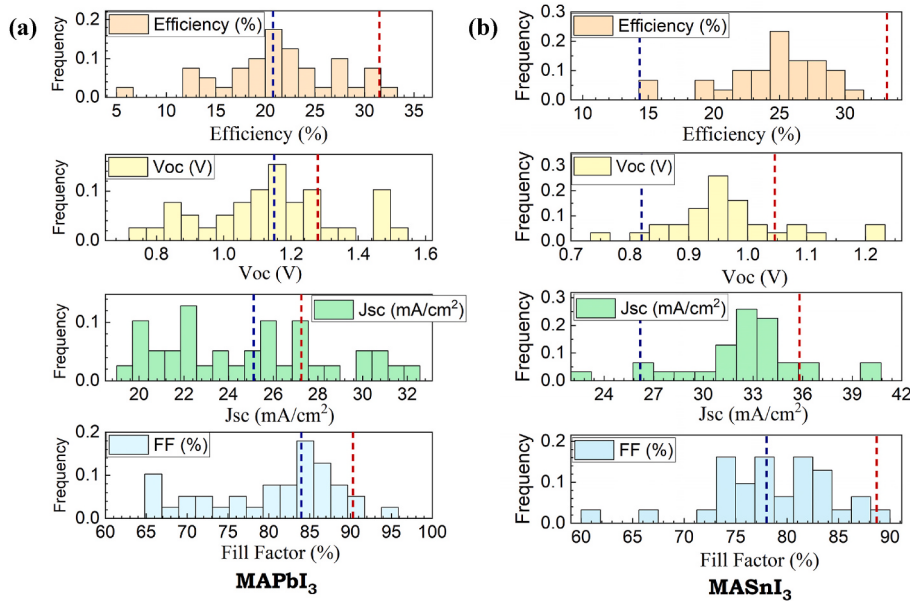


Fig. 3. Reported device performance parameters for (a) MAPbI_3 and (b) MASnI_3 -based based PvSCs using SCAPS-1D. The blue dotted line represents the best externally verified experimental results from PDP, and the red line represents the SQ limit for an absorber with bandgap of 1.55eV and 1.3eV respectively.

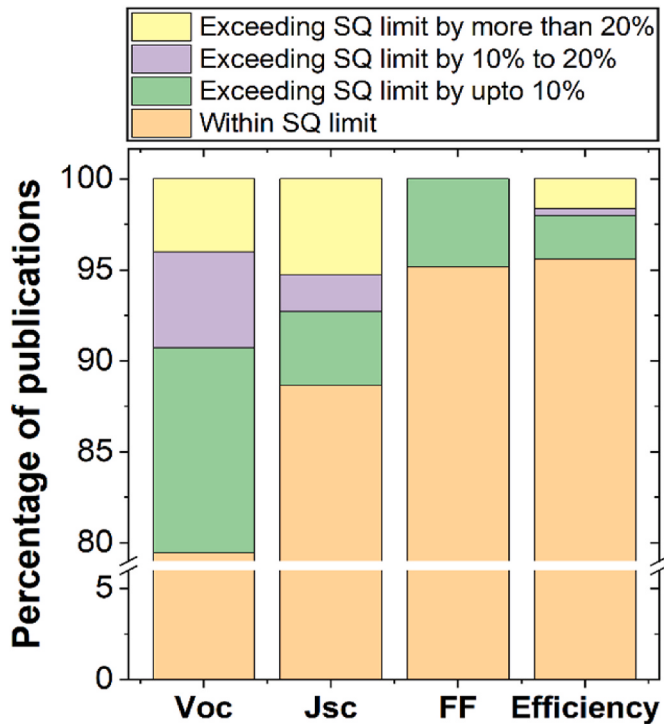


Fig. 4. Reported device performance parameters across all absorber materials for ~250 PvSC architectures surveyed. The SQ limits for the respective reported bandgaps were used for comparison from Ref. [12].

these fundamental properties, used as input for the simulations. For instance, bandgaps of $\text{La}_2\text{NiMnO}_6$ varied from 1.05eV to 1.62eV, while for MAGeI_3 , it ranged from 1.3eV to 1.9eV, with other materials exhibiting similar variability (Fig. 6). This significant lack of consensus on the values of these properties could lead to obtaining simulation results that could remarkably vary from the values that are practically attainable as demonstrated in Section 3.2.

In order to quantify the degree of variation in these parameters, the coefficient of variation was calculated using the following expression,

$$\text{Coefficient of variation} = \frac{\text{Standard Deviation}}{\text{Mean}} \quad (1)$$

The coefficient of variation is a widely used dimensionless statistical metric that provides a normalised measure of dispersion. Unlike standard deviation, this allows for a standardized comparison of relative variability, allowing for a meaningful comparison across different material parameters. It is particularly helpful when the parameters under investigation have different units of measurement or vary in scale. A high coefficient of variation indicates significant variability relative to the mean, suggesting a high degree of dispersion in the dataset. For instance, the variability in a dataset with a standard deviation of 1 and a mean of 10 is higher than that in the dataset with the same standard deviation, but a mean of 100 [26].

Our analyses indicated a considerably higher coefficient of variation for the dielectric permittivity of most materials in the survey, as can be seen in Table 2. This indicates significantly high variability in the value of dielectric permittivity compared to other properties like bandgap and electron affinity. Dielectric permittivity is related to the real component of refractive index (n) by the expression $\epsilon_r = n^2$ [27]. Since refractive index is a function of wavelength, so is dielectric permittivity. The discrepancies in the value of ϵ_r can be attributed to the use of values sourced from different studies disregarding the fact that ϵ_r is a function of wavelength and temperature. Despite this widespread variability in the value of dielectric permittivity for most materials, there seems to be a notable consensus within the community regarding the value of ϵ_r of Spiro-OMeTAD, a widely used HTL, known for enhancing the efficiency of PvSCs [23]. For accurate simulations, it is essential to utilise the value of dielectric permittivity that is valid within the operational wavelength range of the solar cell, as the device performance can remarkably vary due to discrepancies in this parameter, as demonstrated in Fig. 10 (c) in Section 3.2.

Furthermore, the density of states (DOS), which is also an input parameter in SCAPS-1D, and a fundamental thermodynamic quantity influencing the electronic and optical properties of the material, also exhibited substantially high variability. It is primarily determined by the electronic band structure, temperature and chemical composition. Although doping concentrations can modify DOS to a certain extent, the variability in the input parameters is notably large as shown in Fig. 7. Moreover, considerable variability was observed in the DOS, even for

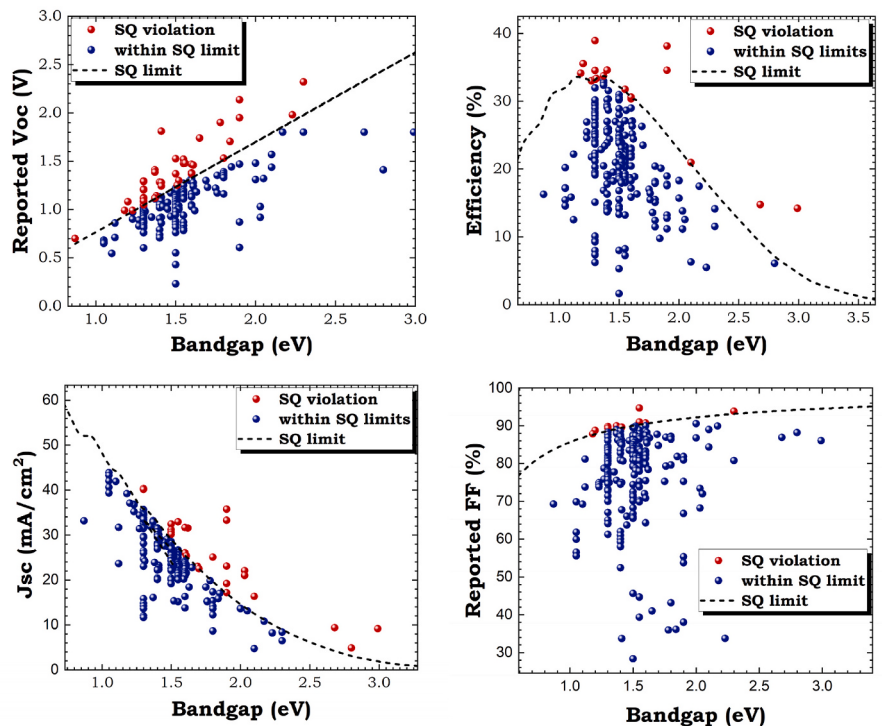


Fig. 5. Reported device performance parameters across all absorber materials for ~250 PvSC architectures surveyed with their reported bandgaps. The dashed black line represents the SQ limit for the respective bandgap for AM1.5G illumination as calculated in reference [12]. The points marked red represent performance metrics that exceed the SQ limit, while the points marked blue represent the points that lie within this theoretical maximum.

Table 1
Overview of survey findings.

		Efficiency	VOC	J _{sc}	Fill Factor
Percentage of publications exceeding best reported experimental efficiency by 20 % or more	MAPbI ₃	25 %	12.8 %	15.4 %	–
	MASnI ₃	93.5 %	35.5 %	80.6 %	–
Percentage of reports exceeding SQ limit	MAPbI ₃	2.5 %	15.4 %	15.4 %	7.7 %
	MASnI ₃	–	13.8 %	6.9 %	–
	All perovskite materials	5.2 %	25.7 %	11.3 %	4.8 %

similar doping concentrations for a given material.

3.2. Unrealistic inputs

The accuracy of simulation results relies strongly on the realism of the input parameters. The primary input parameters taken by SCAPS-1D, along with their default values, have been listed in Table S2 and shown in Figs. S1–S5 in SI. Often, researchers select extremely idealistic values of input parameters to achieve very high efficiencies. These include overly simplified defect models, unrealistically high charge carrier mobilities, excessive doping densities beyond practicality, incorrect density of states and most notably, the unphysically low values of radiative recombination coefficient, which can artificially inflate the simulated performance of the PV device. Once published, these values go into a perpetual cycle, with subsequent research works citing the previous research to justify their choice of input values. In our survey, it

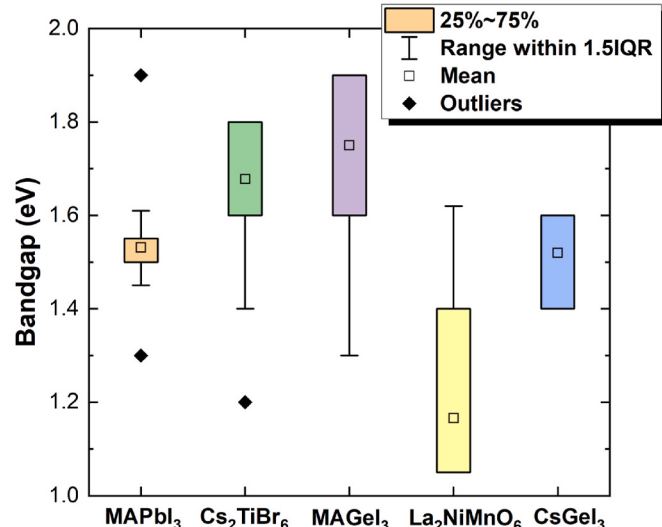


Fig. 6. Variability in the reported bandgap of the absorber layer observed in the survey. Outliers represent points that lie beyond 1.5 Interquartile Range (IQR) from the first (Q1) and third (Q3) quartiles. IQR is defined as the difference between the third and first quartiles, i.e. IQR = Q3–Q1.

was found that in a majority of papers where the reported performance significantly exceeded the best experimental results, unrealistic and unachievable input parameters were used for the simulations. In practice, such unrealistic values could lead to an entirely new substance and possibly result in a different material structure altogether. The wide variability in the parameter values used for MAPbI₃ and MASnI₃ based devices has been illustrated in Fig. S6 in SI.

For most semiconductor materials, mobilities are limited by the scattering of carriers by thermal phonons. The occurrence of band-

Table 2

Coefficients of variation calculated for intrinsic material properties for some common materials found in the survey.

		Bandgap (E_g) (eV)	Electron Affinity (χ) (eV)	Dielectric permittivity (ϵ_r)
MAPbI ₃	Mean	1.52	3.87	15.45
	Std. Dev.	0.052	0.17	10.44
	Coefficient of variation	0.034	0.043	0.68
MASnI ₃	Mean	1.30	4.17	8.28
	Std. Dev.	0.026	0.026	1.193
	Coefficient of variation	0.02	0.006	0.144
Spiro- OMeTAD	Mean	3.008	2.3	3
	Std. Dev.	0.095	0.16	0
	Coefficient of variation	0.03	0.07	0
TiO ₂	Mean	3.18	4.03	18.23
	Std. Dev.	0.14	0.17	23.35
	Coefficient of variation	0.044	0.042	1.28

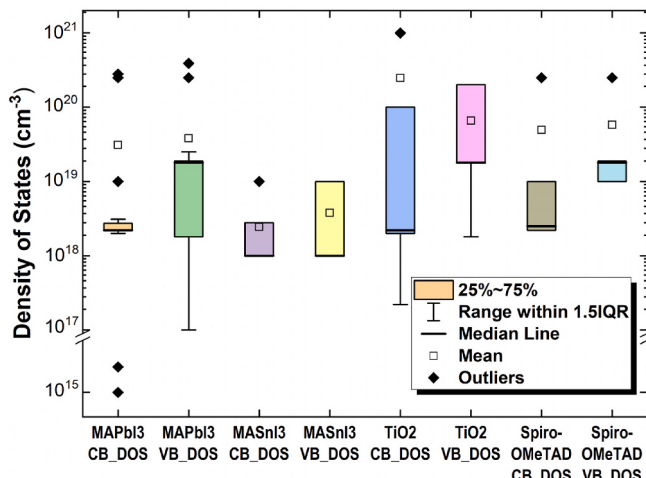


Fig. 7. Variability in the reported effective density of states of the commonly used materials in the survey. Here, CB_DOS refers to the density of states of the conduction band, and VB_DOS refers to the density of states of the valence band.

degeneracy at the valence band edge at the zone center makes interband scattering processes possible, which, along with the higher effective mass of holes, results in hole mobilities that are generally smaller than electron mobilities [25,28]. In the case of perovskite material, an investigation employing density function theory, a range of 5–10 $\text{cm}^2\text{V}^{-1}\text{s}^{-1}$ for electron mobility and 1–5 $\text{cm}^2\text{V}^{-1}\text{s}^{-1}$ for hole mobility was determined, with variations depending on the crystal structure studied and doping level [29]. However, in our survey, numerous publications employing SCAPS-1D considered mobilities substantially higher, with some being as high as even $2000\text{cm}^2\text{V}^{-1}\text{s}^{-1}$ [30,31]. Furthermore, several publications reported hole mobility considerably higher than electron mobility, which necessitates a careful evaluation of the physical validity of the same.

Furthermore, in practice, doping is an extremely challenging and intricate process. For silicon-based photovoltaic cells, being an extensively studied technology, the mechanisms and procedures of doping have been extensively studied and are well documented. However, for perovskite solar cells, unlike silicon, there are very few documented literature sources on this topic. Moreover, the diversity in chemical

compositions and crystalline structures of perovskites further complicates this issue. Each type of perovskite would require a distinct doping approach. One of the most significant challenges with doping is lattice mismatch. Despite these challenges, several publications reported using excessively high doping concentrations (Fig. 8), which may not be physically achievable. Furthermore, high doping concentration can also result in a change in the semiconducting behaviour of the material itself. The effect of using very high doping concentrations on the performance of the device has been studied using the device architecture mentioned in Ref. [21] and illustrated in Fig. S7 in SI. It is quite evident that the use of excessively high doping concentrations can lead to a substantial exaggeration of the performance of the device.

In order to assess the impact of using varied input parameters that deviate from experimentally validated values, a device architecture discussed in the paper referenced as [21] was simulated across a range of input parameters and the effect on the device performance was systematically studied using SCAPS-1D. The input parameters for these simulations were taken from the paper therein and have been described in SI. Although it is acknowledged that varying some of these parameters would render the cell non-physical, this exercise was solely performed to emphasise the necessity of using appropriate input values. The results have been illustrated in Figs. 9–11, and Figs. S7–S10 in SI.

In Fig. 9, it is illustrated that increasing the bandgap of the absorber layer (MASnI₃) results in an increase in the open circuit voltage (V_{oc}). This is because V_{oc} increases linearly with bandgap [32]. However, the short circuit current density (J_{sc}) drops sharply with increasing bandgap of the absorber material. This can be attributed to increased transmission losses as the number of photons with energy greater than the bandgap energy incident on the active layer decreases as bandgap increases. As a result, the number of photons absorbed decreases leading to a decline in the quantum efficiency of the device and a subsequent drop in the value of J_{sc} . Overall, this leads to a decrease in the PCE of the cell. A similar trend is observed when the bandgap of the ETL is increased. This highlights the necessity of entering the appropriate value of bandgap for simulations.

The same exercise was repeated for electron affinity and dielectric permittivity (Fig. 10). It has been found that the efficiency (η) and short circuit current density (J_{sc}) rapidly shoot up from 0.59 % to 24.28 % and from 3.09 mA/cm^2 to 28.45 mA/cm^2 , respectively, when the electron affinity of the ETL is raised from 3.8 eV to 4 eV as illustrated in Fig. 10(a).

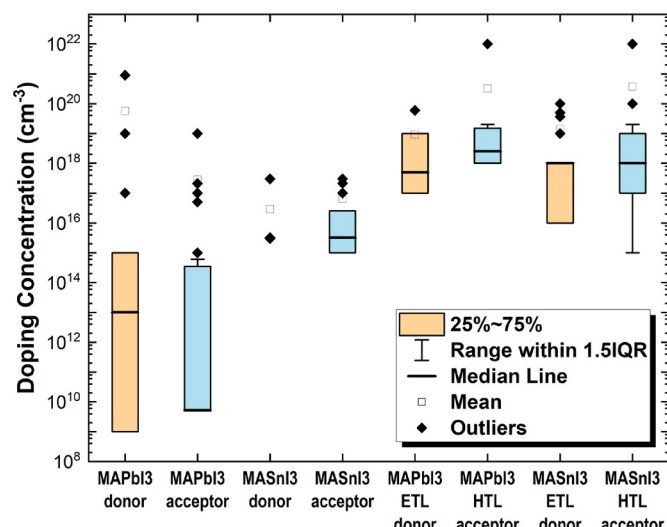


Fig. 8. Variability in the reported shallow uniform doping concentrations observed in the surveyed MAPbI₃ and MASnI₃ based device architectures. Here, 'MAPbI₃ ETL donor' refers to the reported shallow uniform donor doping concentration of the electron transport layer used in the surveyed MAPbI₃-based PvSC, with similar conventions applied for the other materials.

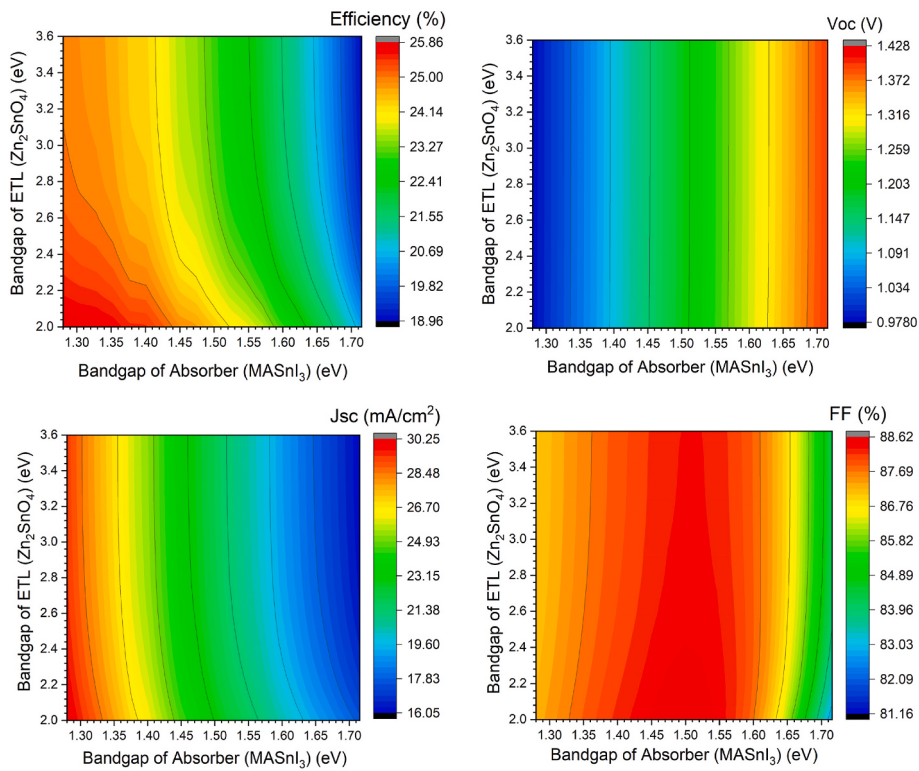


Fig. 9. Dependence of device performance on the bandgap of the absorber layer and ETL for the device architecture discussed in the paper referenced as [21] with input parameters described in Table S1 in SI.

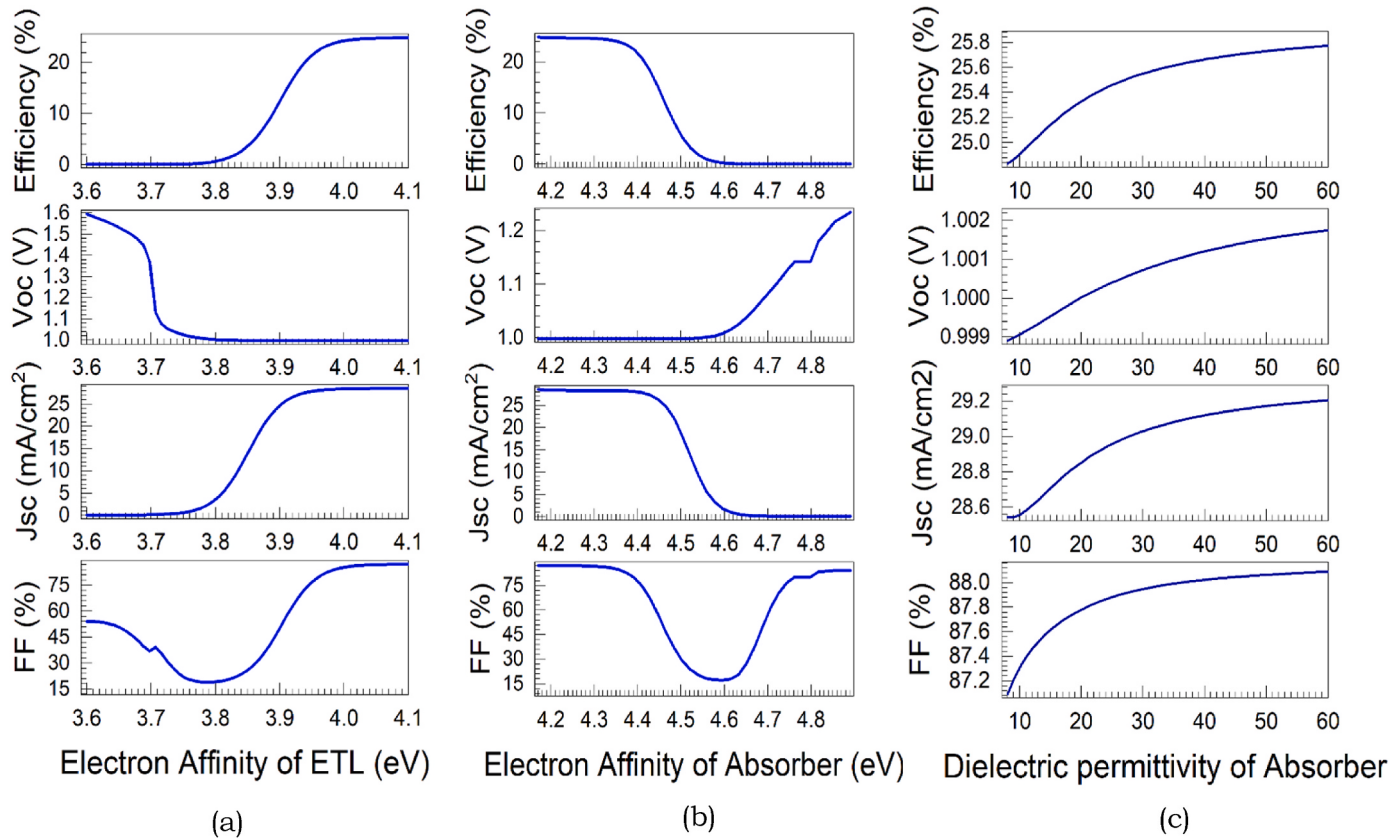


Fig. 10. Dependence of device performance on (a) electron affinity of the ETL, (b) electron affinity of the absorber layer, and (c) dielectric permittivity of the absorber layer for the device architecture discussed in the paper referenced as [21] with input parameters described in Table S1 in SI.

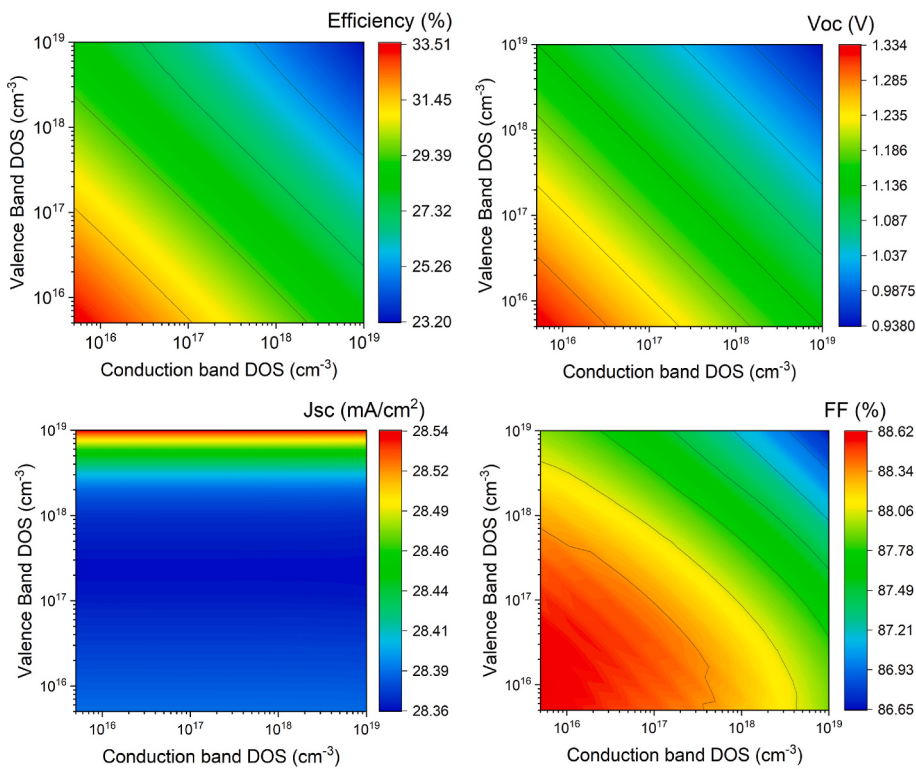


Fig. 11. Dependence of device performance on the effective density of states of the conduction band and valence band of the absorber layer for the device architecture discussed in the paper referenced as [21] with input parameters described in Table S1 in SI.

This can be attributed to the enhanced collection of the photogenerated electrons, at higher electron affinities of the ETL. In contrast, the open circuit voltage (V_{oc}) dropped from 1.6 V to 1V when the electron affinity of the ETL was varied from 3.6eV to 3.8eV, slightly preceding the rise in η and J_{sc} . Conversely, an opposite trend was observed when the electron affinity of the absorber was increased from 4.2eV to 4.8eV (Fig. 10(b)). A decrease in the values of η and J_{sc} was observed, while V_{oc} shot up. Notably, at low electron affinity of the ETL and high electron affinity of the absorber layer, the open circuit voltage even went beyond the SQ limit. Similarly, increasing the dielectric constant of the absorber layer (MASnI₃) from 10 to 30, resulted in a rise in all the four-performance metrics- η , V_{oc} , J_{sc} and FF as can be seen in Fig. 10(c). This highlights the extent of possible discrepancy between the results obtained from electrical modelling using SCAPS-1D and the physically achievable performance if the input parameters are not valid in the range of operation of the photovoltaic device.

Additionally, it was found that η and V_{oc} decrease as the effective DOS of the conduction band and the valence band are increased, as illustrated in Fig. 11. However, the impact of Valence Band DOS was minimal compared to the effect of Conduction Band DOS on the value of J_{sc} . Overall, the efficiency of the device decreases as the DOS increases. In conclusion, from the above analyses, it is quite evident that the repercussions of using values that are not accurate or valid in the operation conditions of the cell can be quite profound. Using input values without verifying their physical validity can not only lead to artificial and unattainable results, but also perpetuates a cycle of misinformation within the scientific community.

In a practical solar cell, parasitic resistances such as series resistance and shunt resistance diminish the overall performance of the solar cell, particularly the fill factor. Series resistance in a PV cell arises primarily from the movement of current through the bulk of the layers in the device, contact resistance between adjacent layers at the interfaces, and the resistance of the top and bottom metal contacts [33]. Shunt resistances, on the other hand, typically arise from defects during

fabrication. At lower shunt resistances, significant power losses can occur due to the presence of an alternate low-resistance path for the photo-generated charge carriers, leading to leakage currents [34]. However, in SCAPS-1D, the default value of series and shunt resistances are set as zero and infinite, respectively [35]. Although SCAPS-1D provides an option for the users to enter custom values of external series and shunt resistance, this option has been rarely utilized in the surveyed studies. Using the default value would lead to an overestimation of the performance of the device compared to the actual performance of the cell. A high-performance PvSC typically has a series resistance of a few ohms and a shunt resistance that ranges from a few kilos to a few mega ohms [36]. In order to underscore the implications of not using realistic values of these parasitic resistances, we conducted simulations by varying the values of series and shunt resistances, as demonstrated in Fig. S10 in SI, for the device architecture described in Ref. [21] with default input parameters described in the Supporting Information. The results indicate that when the value of series resistance is increased, and the shunt resistance is decreased, the performance of the solar cell diminishes remarkably. Notably, the impact of varying series resistance on V_{oc} is minimal compared to the effect of shunt resistance. Therefore, it is necessary for the users to utilise appropriate values of parasitic resistance for simulations. Failing to do so may lead to artificially high device performance metrics.

3.3. Varying parameters while keeping dependent parameters unchanged

As described in Section 3.1, bandgap (E_g), electron affinity (χ) and dielectric permittivity (ϵ_r) are intrinsic properties of a material. However, in numerous studies such as [8,37–40], several fundamental properties, including E_g , χ and ϵ_r , have been optimized to achieve maximum efficiency. This was done by varying the target input parameter, keeping other parameters unchanged. It is essential to recognize that many of these attributes are characteristic to a given material and its crystal structure. Moreover, many of these are

interrelated through fundamental, yet complex, physical relationships [41–44]. Altering one property can have a significant impact on the values of the other parameters. For instance, varying the bandgap could alter the electron affinity and dielectric constant of the material.

As a result, the approach of optimising individual parameters in isolation inevitably leads to the violation of the basic material laws governing the device, rendering the cell non-physical. Using parameter combinations that are not physically possible could lead to getting results that do not reflect the true potential of the device. This may also lead to extreme overestimation of the device performance, as discussed in Section 3.2. In most of these studies, the simulated device performance significantly surpassed the best experimental results, and some even exceeded their respective SQ limits. Therefore, it is imperative to utilise accurate input parameters for simulations using SCAPS-1D and avoid optimization of parameters using SCAPS-1D that could influence other properties of the material.

3.4. Limitation of SCAPS-1D in modelling optical effects

In practice, a significant portion of the incoming radiation is lost due to optical losses in a photovoltaic device. In a typical perovskite solar cell, only ~65 % of the incident light is used to generate excitons in the active layer. Nearly 4 % of the incident light is reflected by the top glass surface, ~14 % is absorbed by the transparent conducting oxide, and ~15 % of the light passes unabsorbed [45]. These inherent losses significantly diminish the overall performance of the cell.

SCAPS-1D can account for reflection and transmission at the two contacts only if these values are explicitly inputted by the user. However, these values are, by default, set as zero and unity, for reflection and transmission, respectively. Moreover, it completely ignores any reflection losses at the intermediate interfaces [35]. However, in practice, a substantial portion of light entering the device is lost as reflection losses at the intermediate interfaces due to refractive index mismatch between the two layers. Although these losses can be calculated using Fresnel's equations [46] using the complex refractive indices of the materials, SCAPS-1D does not account for these as it does not take inputs for the values of the refractive indices of the materials. Therefore, the simulation results would invariably lead to the performance metrics obtained from SCAPS-1D being significantly overestimated than what is physically achievable. The inability of SCAPS-1D to account for optical effects like interference and scattering further undermines its simulation accuracy.

Furthermore, SCAPS-1D uses a very coarse optical absorption model for exciton generation by default. The default absorption model used in SCAPS-1D is the E_g -sqrt model, which is described by the following expression for $h\nu > E_g$ [35],

$$\alpha(h\nu) = \left(\alpha_0 + \frac{\beta_0 E_g}{h\nu} \right) \sqrt{\frac{h\nu}{E_g} - 1} \quad (2)$$

where h is Planck's constant, ν is the frequency of the incident photon, α is the absorption coefficient corresponding to energy $h\nu$ of the incident photon, and E_g represents the bandgap of the material. Here, α_0 and β_0 are constants that can be tuned by the user, if required. For $h\nu < E_g$, α is considered to be zero.

In Fig. 12, we present the absorption profile of MAPbI_3 , computed using the default absorption settings in SCAPS-1D, assuming a bandgap of 1.55eV. This profile has been compared with absorption coefficients reported in the existing literature. It can be inferred from the figure as well as from Equation (2) that the absorption coefficients calculated by the SCAPS-1D model decrease monotonically with increasing wavelength of light. However, in practice, the actual absorption profiles possess intricate features, including peaks and troughs at specific wavelengths, which are intrinsic and characteristic of the material. As can be observed in the figure, the SCAPS-1D model fails to adequately

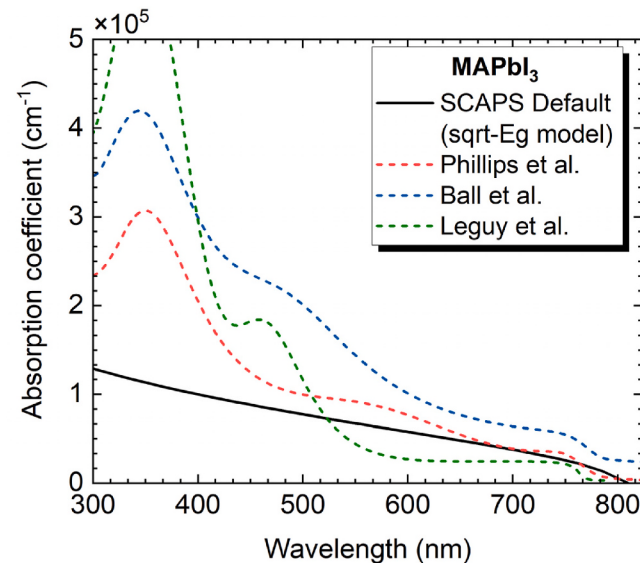


Fig. 12. Comparison of the Absorption coefficients calculated using the SCAPS-1D default ($\text{sqrt-}E_g$) model (black line) and the data reported in the existing literature (dotted lines) for MAPbI_3 [47–49]. The absorption coefficients using $\text{sqrt-}E_g$ model were computed assuming a bandgap of 1.55eV for MAPbI_3 . It is evident that the SCAPS-1D absorption model fails to adequately capture the intricate complexities of the experimentally validated absorption profiles as reported in the literature.

account for these complexities, leading to simulation results that may significantly diverge from the real-world performance of the cell. In addition to the default E_g -sqrt model, there are several other inbuilt absorption models, namely background (constant α), E_g -step, power1, power2, as well as an option to include a sub-bandgap tail, as detailed in the SCAPS-1D manual [35]. However, these alternative models are also subject to the same limitations as described above. Although users can input a more realistic and wavelength-dependent absorption profile as ASCII-files into the software, however, most researchers often use the default settings.

Moreover, the absorption coefficients of perovskite materials also depend on the fabrication methods employed as well as the time elapsed after deposition, primarily due to the inherent stability issues associated with perovskite materials [50]. This underscores the necessity of using appropriate absorption coefficient that consider the specific fabrication technique relevant to the simulations being conducted.

No paper in the survey mentioned inputting any value of reflectance or absorbance for simulations. Moreover, the default AM1.5G spectrum in SCAPS-1D also has several discrepancies compared to the AM1.5G spectrum published by the National Renewable Energy Laboratory (NREL) [51], as demonstrated in Fig. 13, further compounding the issue. While these differences are likely due to the use of fewer data points for computational efficiency and to reduce simulation time, they compromise the reliability and accuracy of the simulation results. Although, the user can input custom illumination spectra from the literature or choose another built-in spectrum with more number of data points, almost always, the default spectrum is used. This can lead to getting results that are far from reality, especially if the absorption region of the active layer coincides with the regions of these discrepancies.

In order to stress on the importance of using the right reflectance value for simulations, SCAPS-1D simulations were performed for varied values of reflectance at the front surface for the PSC device architecture described in the paper [21], and the simulation results have been presented in Fig. 14. As the value of reflectivity is increased from 0 to 10 %, the efficiency of the device correspondingly drops from 24.8 % to 22.2 %, with a decline in J_{sc} from 28.5 mA/cm² to 25.6 mA/cm². Thus, it is necessary to use appropriate values of reflectivity in order to obtain

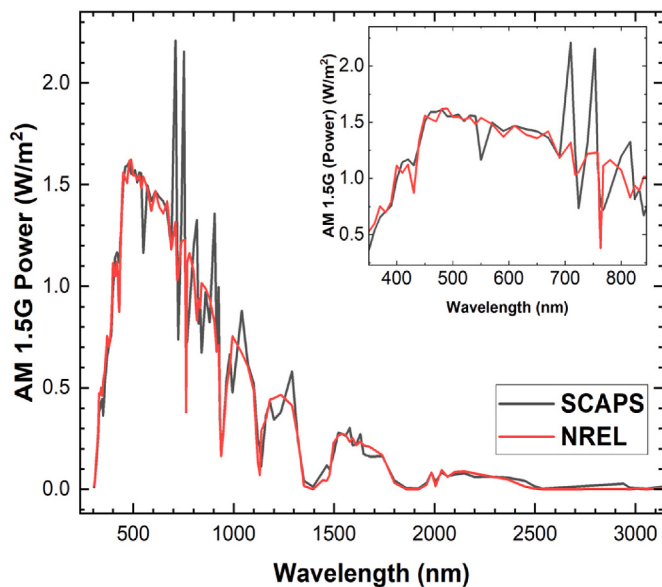


Fig. 13. Discrepancies in the default AM1.5G spectrum in SCAPS-1D compared to the AM1.5G spectrum published by the National Renewable Energy Laboratory (NREL) [51].

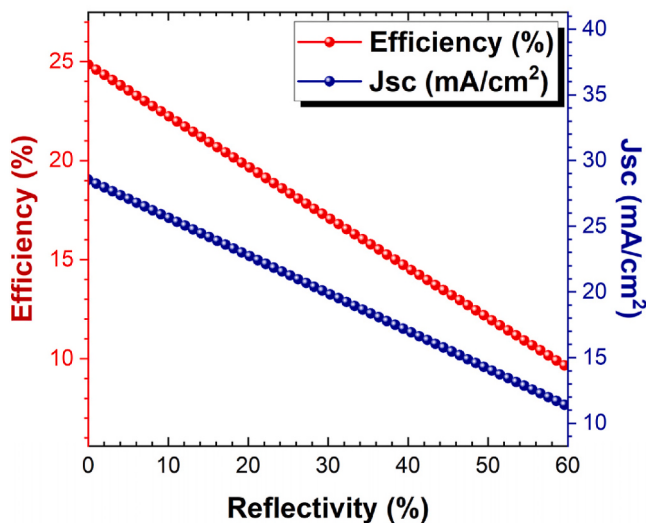


Fig. 14. Impact of reflectivity on Efficiency and Short circuit current density studied using the PSC architecture discussed in the paper referenced as [21] and with default simulation input parameters as described in Table S1 in SI.

accurate and realistic simulation results from SCAPS-1D.

Although none of the above reasons explicitly violate any of the SQ framework assumptions (except for low radiative recombination rate), they could result in unrealistically high results. Therefore, they cannot be directly held responsible for SCAPS-1D simulation results exceeding the theoretical SQ limit.

3.5. Using the default value for radiative recombination coefficient (C_r)

Shockley and Queisser [11,52] argued that, for any cell, even in the dark, with ambient temperature greater than the absolute zero, the surrounding acts as a blackbody and hence emits radiation according to the blackbody (Planck's law),

$$I(\lambda, T) = \frac{2\pi hc^2}{\lambda^5} \cdot \frac{1}{\exp\left(\frac{hc}{\lambda k_B T}\right) - 1} \quad (3)$$

where I represents the power intensity, T represents the temperature of the blackbody, λ represents the wavelength of light, h is Planck's constant while k_B is the Boltzmann constant, and c represents the speed of light.

The solar cell absorbs photons with energy higher than the bandgap energy and generates electron-hole pairs, which subsequently radiatively recombine to re-emit photons with energy equal to the band-gap energy. At equilibrium, these two processes balance each other (detailed balance principle). For any temperature above absolute zero, there is a continual influx of blackbody radiation, leading to an equivalent rate of radiative emission. This imposes a fundamental lower limit to the rate of radiative recombination.

The radiative recombination rate can be expressed as,

$$U_{rad} = C_r (np - n_i^2) \quad (4)$$

where C_r is the radiative recombination coefficient, n and p represent the free electron and free hole densities respectively, and n_i represents the intrinsic carrier density.

Although attributes like defect density, Auger recombination coefficients and SRH recombination coefficients may be set to zero without violating any physical law, the radiative recombination coefficient (C_r) has a fundamental lower limit from the SQ limit formulation and hence cannot be set to zero [11,52]. Since the default value of this coefficient is set to zero in SCAPS-1D, and the user often finds it difficult to obtain a value of C_r from the literature, the user usually keeps the default settings on SCAPS-1D. This invariably leads to a systematic overestimation of the output performance metrics and could result in violation of the SQ limit.

An approximate expression for C_r involving fundamental semiconductor properties can be expressed as [52],

$$C_r = \frac{2\pi c}{N_v N_c} \left(\frac{k_B T}{hc} \right)^3 \left(\frac{E_g}{k_B T} \right)^2 \left(\frac{1}{d} \right) \quad (5)$$

where N_c and N_v represent the density of states in the conduction band and valence band respectively, T represents temperature, h is the Planck's constant while k_B is the Boltzmann constant, and c represents the speed of light. Here, E_g represents the bandgap and d is the thickness of the absorber layer.

Since SCAPS-1D version 3.3.11, there is an option to utilise this value of C_r as expressed in Equation (5) for simulations in the Numerical Panel under 'Numerical Settings' button in the program [35,52], as shown in Fig. S5 in SI. However, the default setting is set as 'Never set Shockley Queisser recombination limit'. Under these settings, the default value of 0 cm³/s shall be used unless specified otherwise by the user. Our analyses indicated that this approximation of C_r as expressed in Equation (5), may not always align closely to the literature value for PvSCs. Therefore, it is strongly recommended to the user to verify the value of C_r from the reliable scientific literature before conducting the simulations.

The impact of using unrealistically low values of C_r has been presented in Fig. 15. Increasing the value of the radiative recombination coefficient of the absorber from 10⁻¹⁰ cm³/s to 10⁻⁹ cm³/s results in a significant drop in the efficiency of the device from 21.08 % to 13.33 %. This is accompanied by a sharp decline in the value of J_{sc} from 25.11 mA/cm² to 17.14 mA/cm², and V_{oc} from 0.97V to 0.93V. Since the variation in the simulated device performance can be quite stark due to even a very slight difference in the value of C_r , it is strongly recommended to use appropriate value of C_r from the literature for carrying out simulations.

Shockley-Read-Hall (SRH) recombination is a defect-mediated non-radiative recombination mechanism that occurs via trap energy levels

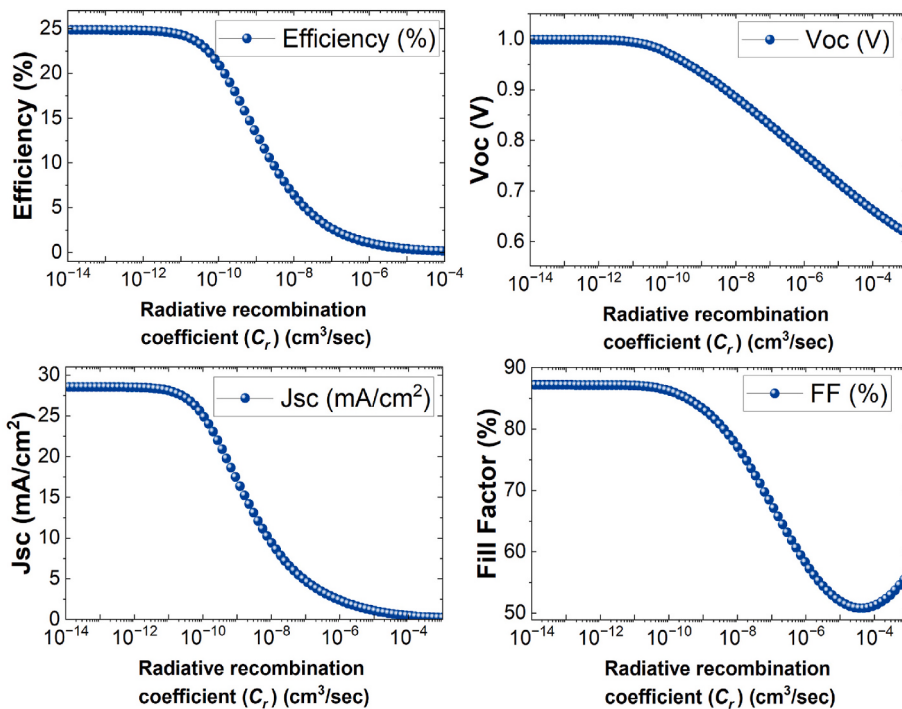


Fig. 15. Dependence of device performance on radiative recombination coefficient of the absorber layer for the device architecture discussed in the paper referenced as [21] using the input simulation parameters discussed in SI.

within the bandgap [53]. The extent of SRH recombination in a solar cell is determined by the defect density. At very low defect density and C_r , the net rate of recombination of charge carriers can be impractically low resulting in inflated device performance which may even surpass the SQ limit, as demonstrated in Fig. 16. This emphasises the necessity of

utilising accurate value of C_r and defect density for simulations as even a slight discrepancy in these values could yield artificial and unachievable results.

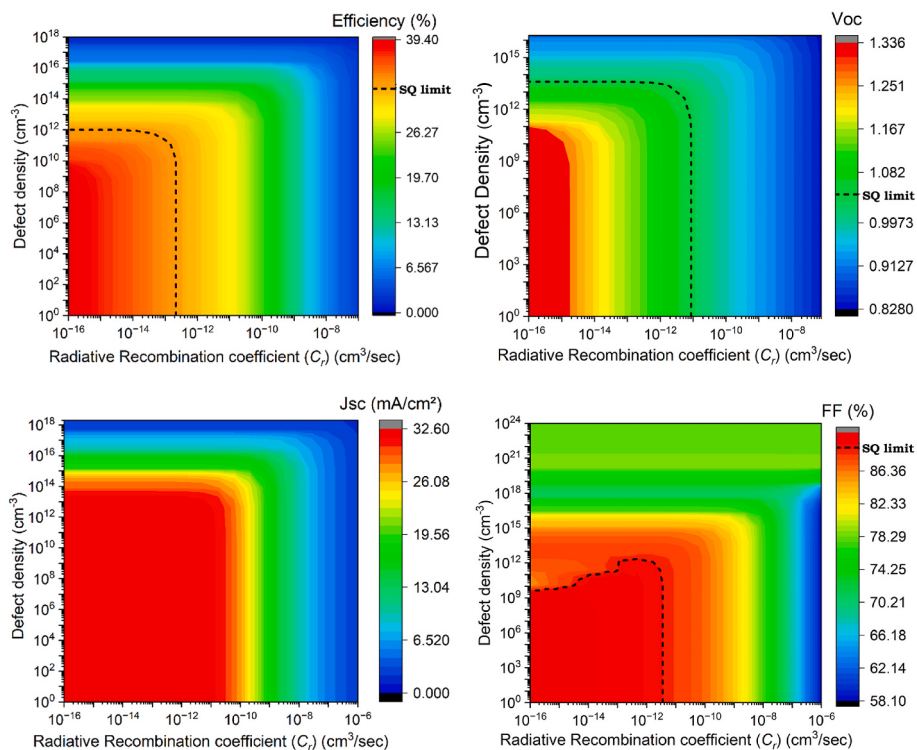


Fig. 16. Dependence of device performance on radiative recombination coefficient and defect density of the absorber layer for the device architecture discussed in the paper referenced as [21] using the input simulation parameters discussed in Table S1 in the Supporting Information. The dotted line represents the SQ limit calculated for a material with a bandgap of 1.3eV for AM1.5G illumination used from the paper referenced as [12].

4. Current challenges in obtaining realistic simulation results using SCAPS-1D

While SCAPS-1D has become an indispensable tool for simulating the electrical performance of PV devices, several challenges continue to impede the accuracy and reliability of the simulation results, as revealed by our analysis of the survey results.

In the context of emerging materials such as perovskites, the major obstacle is the relative scarcity of reliable and experimentally verified data necessary for accurate inputs for simulations, compared to well-established conventional materials like silicon or gallium arsenide. This issue is particularly problematic for newly discovered or novel materials that are currently being explored as potential candidates for PV applications, where critical attribute values, such as carrier mobilities, defect densities, and recombination rates, among others, are either unavailable or inconsistent across different studies. Furthermore, the absence of a consolidated database for these essential parameters compounds problem. A centralised database, compiled from credible sources in the existing literature, would streamline the simulation process and provide standardised parameters that are specific to the material, fabrication methods and operation conditions of the solar cell. Such a resource would not only save time but will also minimise the errors in sourcing data through disparate sources based on varied conditions and fabrication techniques.

Another pervasive issue is the growing trend of prioritising sensational results over methodological rigour which damages the scientific integrity of the community. In the pursuit of obtaining high performance, some researchers overlook critical factors such as recombination rates, parasitic resistances and interface defects. Furthermore, the selective use of data from sources that produce favourable results, disregarding their validity in the conditions of operation of the solar cell, compromises the credibility of SCAPS-1D simulations and leads to the dissemination of inflated and unrealistic device simulations.

A crucial hindrance in obtaining realistic simulation results lies in the inability of SCAPS-1D to account for optical effects and its oversimplified default settings. As of SCAPS-1D version 3.3.11, it does not have the capability to incorporate tools such as the Transfer Matrix Method to take optical losses into account and use the effective intensity of light reaching each infinitesimal layer of the solar cell. For perovskite solar cells where light management plays a crucial role, these inherent limitations of SCAPS-1D can significantly skew the simulation outcomes.

Moreover, the inability of SCAPS-1D to model the instabilities inherent to perovskite materials can also be a challenge while attempting to obtain more realistic simulations. Perovskite materials are known to degrade over time due to various mechanisms such as ion migration, moisture and oxygen ingress, illumination accelerated decomposition, and thermal instability among others [54,55]. SCAPS-1D does not account for these degradation mechanisms and assumes that the material remains stable throughout its operational lifetime. Therefore, it cannot predict long term stability or performance degradation, which remain critical factors in the commercial viability of perovskite solar cells.

Perhaps one of the most fundamental challenges is the widespread lack of thorough reading and knowledge of the SCAPS-1D manual regarding its intended use and inherent limitations. This can result in flawed assumptions, incorrect choice of settings and misinterpretation of the simulation results. A comprehensive understanding of the framework of the software is essential to accurately simulate the performance of any solar cell device, which would reflect its true potential.

5. Recommendations and future perspectives

Based on our analysis of the papers in the survey, we put forth a few recommendations for the entire PV community while performing any simulation using SCAPS-1D.

- i) Varying parameters which could influence other dependent parameters should be avoided. For example, optimization of attributes like bandgap, dielectric constant and electron affinity for maximising device performance should be avoided. Among the parameters that could be varied are the thicknesses of the constituent layers and doping concentration to a certain limit.
- ii) Only parameter values that are physically and practically achievable and valid in the operation conditions of the solar cell must be used. As many material-specific attributes depend on the fabrication methods employed, it is essential to use data corresponding to a specific fabrication process only. Furthermore, it is strongly recommended to declare the fabrication process on which the simulations are based on while reporting the results. In addition, it is crucial to enter appropriate radiative recombination coefficient (C_r) for SCAPS-1D simulations. Failure to do so was identified as the primary reason behind the violation of SQ limit among the papers surveyed. Therefore, it should be mandatory to report the values of the radiative recombination coefficient utilized for simulations in any publication reporting SCAPS-1D simulation results.
- iii) A few updates to SCAPS-1D are desirable to enhance its optical modelling capabilities. These include incorporating scattering and interface phenomena, as well as accounting for reflection losses at intermediate interfaces. This can be accomplished by taking inputs for the wavelength-dependent complex refractive index of each material, i.e. n-k values. Furthermore, several phenomena outside the SQ framework, such as multiple exciton generation, photon up-conversion, intermediate band photovoltaics, hot carrier cells and photon recycling, have come up in recent times, which could also be integrated into SCAPS-1D.
- iv) SCAPS-1D should, by default, warn the user of any unrealistic and impractical inputs entered by the user, especially for the radiative recombination coefficient, before proceeding with the simulations. Furthermore, a comprehensive simulation report with complete details of the device architecture and attribute values could be generated by the software. Including this report as supplementary information would lead to higher credibility of the reported simulation values and minimise inadvertent reporting of wrong values like the ones we found in the survey.
- v) As the variation in the simulated device performance could be quite profound due to even small errors in some input parameters such as electron affinity and radiative recombination coefficient (C_r), SCAPS-1D could theoretically compute the error margins in the simulated performance based on the individual parameter uncertainties and report it as uncertainties in the simulated performance.
- vi) We propose the incorporation of stability analysis tools into SCAPS-1D, in order to model the stability of perovskite solar cells by taking into account some inherent degradation mechanisms such as ion-migration, moisture sensitivity and illumination accelerated degradation among others.
- vii) We propose that a standardised and universally accepted open-source database be established and maintained for parameters such as bandgap and electron affinity across all materials. This database would serve as a single, uniform and consolidated source for input parameters for SCAPS-1D simulations as well as any other scientific analyses dependent on these values. Ideally, SCAPS-1D should directly connect to this database via the internet to retrieve all electrical and optical properties of the material. This would help to prevent the inconsistencies observed in the input values during our survey.
- viii) Moreover, making SCAPS-1D open-source could allow harnessing the collective capability of the entire PV community to enhance the accuracy of SCAPS-1D in modelling photovoltaic cells. Collaborative efforts in building standardised datasets, refining material models, and introducing more accurate functionalities

could transform SCAPS-1D into an indispensable part of the global PV research infrastructure.

5.1. Standard simulation protocol

- Ensure that the input parameters, including C_r , are obtained from reliable scientific literature and are valid in the operation conditions of the PV cell. Verify that they are within physical limits.
- Systematically report all input parameters, especially C_r and defect density in the publication.
- If possible, obtain an effective transmitted spectrum of light as a function of wavelength reaching the absorber layer via optical modelling (Transfer Matrix Method), and input the modified AM1.5G spectrum into SCAPS-1D for electrical simulations.
- Input appropriate wavelength-dependent absorption profile for the absorber layer into SCAPS-1D.
- Ensure that the simulation results adhere to SQ limits. If the results show significant deviations from the best experimental results, provide an explanation for this discrepancy. Is it because of overly idealistic or oversimplified input parameters, or does it indicate potential for experimental advancements in PV cell technology?

Looking forward, the future of SCAPS-1D and its role in PV research holds great potential as new materials and advanced device architectures continue to emerge. The development of hybrid simulation tools that can perform electrical and optical modelling in conjunction, which would enhance simulation accuracy, is inevitable in the near future. This would allow for detailed studies of light management strategies that hold paramount importance for emerging PV technologies such as multi-junction, tandem and bifacial solar cells. The extension of SCAPS-1D capabilities to accommodate new and advanced architectures would ensure its continued relevance and utility in the fast-evolving landscape of PV technology.

Incorporating models to account for degradation mechanisms such as ion migration, thermal instability, and moisture-induced degradation along with environmental factors would allow researchers to model and predict the long-term performance of perovskite solar cells, addressing one of the key bottlenecks for their commercialisation. The establishment of a global standardised and open-source database for material properties is essential. This would minimise inconsistencies in input parameters and act as a reliable source for experimentally verified data across materials and fabrication strategies. By directly integrating with SCAPS-1D, such a database would streamline the simulation process and enhance the credibility of the reported results. With the ever-increasing pool of data and the emergence of advanced computational capabilities in recent times, the pursuit of new, stable and more efficient device architectures can be accelerated. By systematically exploring combinations of different material layers using material parameters from the centralised database, and applying realistic models for simulations, device architectures can be optimized for high performance as well as longer operational lifetime. The use of Artificial Intelligence and Machine Learning can further accelerate this search. In the long term, the open sourcing of SCAPS-1D would foster global collaboration, allowing experts from diverse disciplines to contribute towards refining and enhancing the accuracy and realism of the simulation results.

6. Conclusion

SCAPS-1D is a very powerful and popular tool used for simulating the performance of solar cell devices and offers valuable insights that aid in the advancement of PV technology. Our survey uncovered a disturbing trend of overexaggerated device performance metrics being frequently reported, even in prestigious journals, via electrical simulations using SCAPS-1D. From this study, we conclude, among other things, that it is essential to ensure that the input parameters, especially the radiative

recombination rate, are realistic and within physical limits. Failure to do so may result in simulations yielding unrealistic outputs and perpetuate a cycle of misinformation in the scientific community. Moreover, optimising fundamental and intrinsic material properties like electron affinity and bandgap, disregarding their potential interdependence with other parameters, further compounds the issue. Further, the optical limitations of SCAPS-1D in accounting for scattering and interference effects and, most importantly, reflection losses at intermediate interfaces have further exacerbated this issue. The results obtained from SCAPS-1D simulations must always be taken with caution as there would inevitably remain a discrepancy between the theoretical results and practically attainable cell performance. It must be realised that the accuracy of the results obtained from any software are highly dependent on the realism and validity of the input parameters, as well as the assumptions and algorithms used. Thus, it is imperative for the research community to exercise discernment while interpreting any theoretical result. Such practices can only be avoided via collective effort and consensus in the community. Since there is significant pressure on researchers to achieve superior device performance that can lead to publication in high-impact journals and secure funding, it is ever more important that researchers and reviewers alike are well-versed in the validity of simulation methods and understand the level of potential error that may be introduced by the simulation procedures. It is imperative to prioritise new scientific insights rather than sensational and flashy results. The entire research community, including authors, reviewers, and editors, must work together to prioritise accurate reporting. They should be vigilant in assessing the validity of reported efficiencies and ensure that authors adhere to standardised simulation wherever applicable and necessary. Failure to do so would result in the loss of credibility of the field and stalling of the progress of genuine scientific pursuits. By addressing these issues through a culture that values accuracy over sensationalism, the solar cell research community can ensure that reported efficiencies are reliable, reproducible, and genuinely reflective of technological progress.

CRediT authorship contribution statement

Abhisek Saidarsan: Writing – original draft, Visualization, Formal analysis, Data curation. **Satyabrata Guruprasad:** Visualization. **Ashish Malik:** Formal analysis. **Pilik Basumatary:** Validation, Supervision. **Dhriti Sundar Ghosh:** Visualization, Validation, Supervision, Conceptualization.

Funding sources

This research did not receive any specific grant from funding agencies in the public, commercial, or not-for-profit sectors.

Declaration of competing interest

The authors declare that they have no known competing financial interests or personal relationships that could have appeared to influence the work reported in this paper.

Acknowledgements

The authors would like to thank Dr. Marc Burgelman for providing access to SCAPS-1D software for carrying out the simulations discussed in this paper.

Appendix A. Supplementary data

Supplementary data to this article can be found online at <https://doi.org/10.1016/j.solmat.2024.113230>.

Data availability

Data shall be made available on reasonable request to the corresponding authors.

References

- [1] N.S. Lewis, D.G. Nocera, Powering the planet: chemical challenges in solar energy utilization, *Proc. Natl. Acad. Sci. USA* 103 (43) (2006) 15729–15735, <https://doi.org/10.1073/pnas.0603395103>.
- [2] M.A. Green, et al., Solar cell efficiency tables (Version 63), *Prog. Photovoltaics Res. Appl.* 32 (1) (2024) 3–13, <https://doi.org/10.1002/pip.3750>.
- [3] A. Niemegeers, M. Burgelman, Numerical modelling of AC-characteristics of CdTe and CIS solar cells, in: Conference Record of the Twenty Fifth IEEE Photovoltaic Specialists Conference - 1996, 1996, pp. 901–904, <https://doi.org/10.1109/PVSC.1996.564274>.
- [4] M. Burgelman, P. Nollet, S. Degraeve, Modelling polycrystalline semiconductor solar cells, *Thin Solid Films* 361–362 (2000) 527–532, [https://doi.org/10.1016/S0040-6090\(99\)00825-1](https://doi.org/10.1016/S0040-6090(99)00825-1).
- [5] A. Kojima, K. Teshima, Y. Shirai, T. Miyasaka, Organometal halide perovskites as visible-light sensitizers for photovoltaic cells, *J. Am. Chem. Soc.* 131 (17) (May 2009) 6050–6051, <https://doi.org/10.1021/ja809598r>.
- [6] P. Basumatary, P. Agarwal, A short review on progress in perovskite solar cells, *Mater. Res. Bull.* 149 (2022) 111700, <https://doi.org/10.1016/j.materresbull.2021.111700>.
- [7] M. Giannouli, Current status of emerging PV technologies: a comparative study of dye-sensitized, organic, and perovskite solar cells, *Int. J. Photoenergy* 2021 (1) (2021) 6692858, <https://doi.org/10.1155/2021/6692858>.
- [8] X. Meng, et al., Optimization of germanium-based perovskite solar cells by SCAPS simulation, *Opt. Mater.* 128 (2022) 112427, <https://doi.org/10.1016/j.optmat.2022.112427>.
- [9] X. Liu, et al., An optimization of Cs₂TiBr₆ perovskite solar cell using SCAPS-1D simulation based on genetic algorithm, *Can. J. Chem. Eng.* n/a (May 2024), <https://doi.org/10.1002/cjce.25315> n/a.
- [10] M. Ghaleb, A. Arrar, Z. Touaa, Optimization and performance analysis of a TiO₂/i-CH₃NH₃SnBr₃/CsPbI₃/Al(BSF) heterojunction perovskite solar cell for enhanced efficiency, *ACS Omega* 8 (40) (Sep. 2023) 37011–37022, <https://doi.org/10.1021/acsomega.3c03891>.
- [11] W. Shockley, H.J. Queisser, Detailed balance limit of efficiency of p-n junction solar cells, *J. Appl. Phys.* 32 (3) (Jun. 1961) 510–519, <https://doi.org/10.1063/1.1736034>.
- [12] S. Rühle, Tabulated values of the Shockley–Queisser limit for single junction solar cells, *Sol. Energy* 130 (2016) 139–147, <https://doi.org/10.1016/j.solener.2016.02.015>.
- [13] P. Krogsstrup, et al., Single-nanowire solar cells beyond the Shockley–Queisser limit, *Nat. Photonics* 7 (4) (2013) 306–310, <https://doi.org/10.1038/nphoton.2013.32>.
- [14] J.E. Spanier, et al., Power conversion efficiency exceeding the Shockley–Queisser limit in a ferroelectric insulator, *Nat. Photonics* 10 (9) (2016) 611–616, <https://doi.org/10.1038/nphoton.2016.143>.
- [15] Y. Chen, et al., Multiple exciton generation in tin-lead halide perovskite nanocrystals for photocurrent quantum efficiency enhancement, *Nat. Photonics* 16 (7) (2022) 485–490, <https://doi.org/10.1038/s41566-022-01006-x>.
- [16] M. Li, et al., Low threshold and efficient multiple exciton generation in halide perovskite nanocrystals, *Nat. Commun.* 9 (1) (2018) 4197, <https://doi.org/10.1038/s41467-018-06596-1>.
- [17] Y.H. Lee, Beyond the Shockley–Queisser limit: exploring new frontiers in solar energy harvest, *Science* 383 (6686) (1979) eado4308, <https://doi.org/10.1126/science.ada04308>, 2024.
- [18] C.A. Nelson, N.R. Monahan, X.-Y. Zhu, Exceeding the Shockley–Queisser limit in solar energy conversion, *Energy Environ. Sci.* 6 (12) (2013) 3508–3519, <https://doi.org/10.1039/C3EE42098A>.
- [19] O.E. Semonin, et al., Peak external photocurrent quantum efficiency exceeding 100% via MEG in a quantum dot solar cell, *Science* 334 (6062) (1979) 1530–1533, <https://doi.org/10.1126/science.1209845>, 2011.
- [20] T.J. Jacobsson, et al., An open-access database and analysis tool for perovskite solar cells based on the FAIR data principles, *Nat. Energy* 7 (1) (2022) 107–115, <https://doi.org/10.1038/s41560-021-00941-3>.
- [21] N.K. Sinha, D.S. Ghosh, A. Khare, Highly efficient, low-cost, lead-free bifacial perovskite solar cells: a designing strategy through simulation, *Materials* 4 (2024) 100219, <https://doi.org/10.1016/j.nxmate.2024.100219>.
- [22] Z. Yao, W. Zhao, S. Frank Liu, Stability of the CsPbI₃ perovskite: from fundamentals to improvements, *J. Mater. Chem. A* 9 (18) (2021) 11124–11144, <https://doi.org/10.1039/DITA01252E>.
- [23] L. Nakka, Y. Cheng, A.G. Aberle, F. Lin, Analytical review of spiro-OMeTAD hole transport materials: paths toward stable and efficient perovskite solar cells, *Adv. Energy Sustain. Res.* 3 (8) (2022) 2200045, <https://doi.org/10.1002/aesr.202200045>.
- [24] W. Bulowski, et al., Optimization of the ETL titanium dioxide layer for inorganic perovskite solar cells, *J. Mater. Sci.* 59 (17) (2024) 7283–7298, <https://doi.org/10.1007/s10853-024-09581-w>.
- [25] C. Kittel, P. McEuen, *Introduction to Solid State Physics*, Wiley, 2018 [Online]. Available: <https://books.google.co.in/books?id=nNpVEAAQBAJ>.
- [26] V. Khare, C. Khare, S. Nema, P. Baredar, Chapter 2 - data visualization and descriptive statistics of solar energy system, in: V. Khare, C. Khare, S. Nema, P. Baredar (Eds.), *Decision Science and Operations Management of Solar Energy Systems*, Academic Press, 2023, pp. 33–75, <https://doi.org/10.1016/B978-0-323-85761-1.00002-0>.
- [27] M.T. Sebastian, Chapter two - measurement of microwave dielectric properties and factors affecting them, in: M.T. SEBASTIAN (Ed.), *Dielectric Materials for Wireless Communication*, Elsevier, Amsterdam, 2008, pp. 11–47, <https://doi.org/10.1016/B978-0-08-045330-9.00002-9>.
- [28] P. Würfel, U. Würfel, Physics of solar cells: from basic principles to advanced concepts, in: No Longer Used, Wiley, 2016 [Online]. Available: <https://books.google.co.in/books?id=UOpbDAAQBAJ>.
- [29] C. Motta, F. El-Mellouhi, S. Sanvitto, Charge carrier mobility in hybrid halide perovskites, *Sci. Rep.* 5 (1) (2015) 12746, <https://doi.org/10.1038/srep12746>.
- [30] E.A. Nyiekaa, T.A. Aika, E. Danladi, C.E. Akhabue, P.E. Orukpe, Simulation and optimization of 30.17% high performance N-type TCO-free inverted perovskite solar cell using inorganic transport materials, *Sci. Rep.* 14 (1) (2024) 12024, <https://doi.org/10.1038/s41598-024-62882-7>.
- [31] P.K. Patel, Device simulation of highly efficient eco-friendly CH₃NH₃SnI₃ perovskite solar cell, *Sci. Rep.* 11 (1) (2021) 3082, <https://doi.org/10.1038/s41598-021-82817-w>.
- [32] C. B. Honsberg and Bowden S.G., “Open Circuit Voltage,” *Photovoltaics Educ. Website*. Accessed: July. 10, 2024. [Online]. Available: <https://www.pveducation.org/pvcdrom/solar-cell-operation/open-circuit-voltage>.
- [33] C. B. Honsberg and S. G. Bowden, “Series Resistance,” *Photovoltaics Educ. Website*. Accessed: July. 31, 2024. [Online]. Available: <https://www.pveducation.org/g/pvcdrom/solar-cell-operation/series-resistance>.
- [34] C. B. Honsberg and S. G. Bowden, “Shunt Resistance,” *Photovoltaics Educ. Website*. Accessed: July. 31, 2024. [Online]. Available: <https://www.pveducation.org/pvcdrom/solar-cell-operation/shunt-resistance>.
- [35] M. Burgelman, K. Decock, A. Niemegeers, J. Verschraegen, and S. Degraeve, “SCAPS manual,” University of Gent: Gent, Belgium, Sep. 2023, Accessed: June. 12, 2024. [Online]. Available: <https://scaps.elis.ugent.be/SCAPS/20manual/20most/20recent.pdf>.
- [36] M.A. Green, et al., Solar cell efficiency tables (version 62), *Prog. Photovoltaics Res. Appl.* 31 (7) (2023) 651–663, <https://doi.org/10.1002/pip.3726>.
- [37] A. Singh, et al., Enhancing the performance of lead-free La₂NiMnO₆ double perovskite solar cells through SCAPS-1D optimization, *J. Opt.* (2023), <https://doi.org/10.1007/s12596-023-01527-w>.
- [38] H. Dixit, et al., A theoretical exploration of lead-free double perovskite La₂NiMnO₆ based solar cell via SCAPS-1D, *Opt. Mater.* 131 (2022) 112611, <https://doi.org/10.1016/j.optmat.2022.112611>.
- [39] J. Song, et al., Numerical simulation and performance optimization of all-inorganic CsGeI₃ perovskite solar cells with stacked ETLs/C60 by SCAPS device simulation, *Mater. Today Commun.* 38 (2024) 108587, <https://doi.org/10.1016/j.mtcomm.2024.108587>.
- [40] M. Kumar, A. Raj, A. Kumar, A. Anshul, Theoretical evidence of high power conversion efficiency in double perovskite solar cell device, *Opt. Mater.* 111 (2021) 110565, <https://doi.org/10.1016/j.optmat.2020.110565>.
- [41] Y. Dong, R. Zhu, Y. Jia, Linear relationship between the dielectric constant and band gap in low-dimensional mixed-halide perovskites, *J. Phys. Chem. C* 125 (27) (2021) 14883–14890, <https://doi.org/10.1021/acs.jpcc.1c01576>.
- [42] H. Lu, X. Meng, Correlation between band gap, dielectric constant, Young's modulus and melting temperature of GaN nanocrystals and their size and shape dependences, *Sci. Rep.* 5 (1) (2015) 16939, <https://doi.org/10.1038/srep16939>.
- [43] A.C. Sharma, Size-dependent energy band gap and dielectric constant within the generalized Penn model applied to a semiconductor nanocrystallite, *J. Appl. Phys.* 100 (8) (Jul. 2006) 84301, <https://doi.org/10.1063/1.2357421>.
- [44] E. Trushin, M. Betzinger, S. Blügel, A. Görling, Band gaps, ionization potentials, and electron affinities of periodic electron systems via the adiabatic-connection fluctuation-dissipation theorem, *Phys. Rev. B* 94 (7) (Aug. 2016) 75123, <https://doi.org/10.1103/PhysRevB.94.075123>.
- [45] D.-L. Wang, H.-J. Cui, G.-J. Hou, Z.-G. Zhu, Q.-B. Yan, G. Su, Highly efficient light management for perovskite solar cells, *Sci. Rep.* 6 (1) (2016) 18922, <https://doi.org/10.1038/srep18922>.
- [46] A. Morales-Acevedo, R. Bernal-Correa, Chapter Five - optical design of perovskite solar cells, in: S. Sundaram, V. Subramanian, R.P. Raffaele, M.K. Nazeeruddin, A. Morales-Acevedo, M.B. Navarro, A.F. Hepp (Eds.), *Solar Cell Engineering*, Elsevier, 2024, pp. 183–194, <https://doi.org/10.1016/B978-0-323-90188-8.00011-7>. *Photovoltaics Beyond Silicon*.
- [47] A.M.A. Leguy, et al., Reversible hydration of CH₃NH₃PbI₃ in films, single crystals, and solar cells, *Chem. Mater.* 27 (9) (May 2015) 3397–3407, <https://doi.org/10.1021/acs.chemmater.5b00660>.
- [48] L.J. Phillips, et al., Dispersion relation data for methylammonium lead triiodide perovskite deposited on a (100) silicon wafer using a two-step vapour-phase reaction process, *Data Brief* 5 (2015) 926–928, <https://doi.org/10.1016/j.dib.2015.10.026>.
- [49] J.M. Ball, et al., Optical properties and limiting photocurrent of thin-film perovskite solar cells, *Energy Environ. Sci.* 8 (2) (2015) 602–609, <https://doi.org/10.1039/C4EE03224A>.
- [50] P. Basumatary, P. Agarwal, Two-step fabrication of \$\$.hbox {MAPbI}_{3}\$\$ perovskite thin films with improved stability, *Bull. Mater. Sci.* 42 (6) (2019) 268, <https://doi.org/10.1007/s12034-019-1959-1>.
- [51] NREL (National Renewable Energy Laboratory). Reference Air Mass 1.5 Spectra, NREL Website. Accessed: July. 31, 2024. [Online]. Available: <https://www.nrel.gov/grid/solar-resource/spectra-am1.5.html>.

- [52] M. Burgelman, Implementing the Shockley-Queisser efficiency limit in SCAPS [Online]. Available: https://scaps.elis.ugent.be/SCAPS/20Application/20Note/20_Shockley-Queisser/20limit.pdf, 2023. (Accessed 15 June 2024).
- [53] C. B. Honsberg and S. G. Bowden, "Types of Recombination," Photovoltaics Educ. Website. Accessed: July. 15, 2024. [Online]. Available: <https://www.pveducation.org/pvcdrom/pn-junctions/types-of-recombination>.
- [54] D. Wang, M. Wright, N.K. Elumalai, A. Uddin, Stability of perovskite solar cells, Sol. Energy Mater. Sol. Cell. 147 (2016) 255–275, <https://doi.org/10.1016/j.solmat.2015.12.025>.
- [55] T.A. Chowdhury, Md A. Bin Zafar, Md Sajjad-Ul Islam, M. Shahinuzzaman, M. A. Islam, M.U. Khandaker, Stability of perovskite solar cells: issues and prospects, RSC Adv. 13 (3) (2023) 1787–1810, <https://doi.org/10.1039/D2RA05903G>.

A Critical Review of Unrealistic Results in SCAPS-1D Simulations: Causes, Practical Solutions and Roadmap Ahead

Abhisek Saidarsan^{a}, Satyabrata Guruprasad^b, Ashish Malik^b, Pilik Basumatary^b,
Dhriti Sundar Ghosh^{b†}*

^aIndian Institute of Science Education and Research, Pune, India

*^bThin-film and Photovoltaics Laboratory, Department of Physics, Indian Institute of Technology
Dharwad, Dharwad, India*

*Corresponding authors: *abhisek.saidarsan@students.iiserpune.ac.in, †dhriti.ghosh@iitdh.ac.in*

SUPPORTING INFORMATION

• METHODOLOGY

Electrical Modelling by Numerical Simulations via SCAPS-1D

SCAPS-1D numerically solves a system of three fundamental coupled differential equations, namely, Poisson's equation and the continuity equations for electrons and holes [3],[4]. These equations are essential for simulating the performance of the device by electrical modelling and can be expressed as follows [21],[47],

$$-\frac{d^2\psi}{dx} = \frac{d\xi}{dx} = \frac{\rho}{\epsilon} = \frac{q}{\epsilon}(p(x) - n(x) + N_D^+ - N_A^- - n_t(x) + p_t(x)) \quad (A1)$$

$$\frac{dn}{dt} = \frac{1}{q} \frac{dJ_n}{dx} - (U - G) \quad (A2)$$

$$\frac{dp}{dt} = -\frac{1}{q} \frac{dJ_p}{dx} - (U - G) \quad (A3)$$

where ψ is the electrostatic potential, ξ is the electric field, ρ is the charge density, q is the electronic charge, and ϵ is the permittivity of the material. p and n denote the density of holes and electrons, respectively, and N_D^+ and N_A^- represent the donor and acceptor concentrations. n_t and p_t represent the trapped electron and hole densities. U and G are the recombination and generation rates. J_n is the electron current density and J_p represents the hole current density and are given by the following transport equations [1]:

$$J_n = q\mu_n n \xi + qD_n \frac{dn}{dx} \quad (A4)$$

$$J_p = q\mu_p p \xi + qD_p \frac{dp}{dx} \quad (A5)$$

where μ_e is the mobility of the electron, μ_p is the mobility of holes, while D_p and D_n are the diffusivities of holes and electrons, respectively.

- The impact of using unrealistic parameters and optical limitations of SCAPS-1D on the device performance was investigated by performing simulations on a device architecture referenced in the paper [21] using the input parameters mentioned therein and using the default AM1.5G spectrum in SCAPS-1D. These parameter values were specifically chosen to illustrate the extent of discrepancies between practically achievable results and those obtained through simulations. **It is essential to clarify that we neither endorse nor validate the input parameters mentioned in the referenced paper.** We recognize that there are several oversights in the provided parameter set. For instance, the reported hole mobility of Zn_2SnO_4 is considerably higher than the electron mobility, which demands a careful evaluation of the physical validity of the same.

Table S1: Input parameters used for analysing the impact of variation in input parameters on the device performance

Device Architecture: Glass/FTO/ Zn_2SnO_4 /MASnI₃/MAM

Parameter	FTO	MAM	MASnI ₃	Zn_2SnO_4
Thickness (nm)	50	100	500	300
E_g (eV)	3.5	3	1.3	3.67
χ (eV)	4.4	2.3	4.17	4.18
Dielectric permittivity (ϵ_r)	9	4.5	6.5	9
DOS _{CB} (cm ⁻³)	2×10^{18}	2.2×10^{18}	1×10^{18}	2.2×10^{18}
DOS _{VB} (cm ⁻³)	2×10^{18}	1.8×10^{19}	1×10^{19}	1.8×10^{19}
Electron Thermal velocity (cm/sec)	10^7	10^7	10^7	10^7
Hole Thermal velocity (cm/sec)	10^7	10^7	10^7	10^7
Electron mobility (cm ² V ⁻¹ s ⁻¹)	2000	150	1.6	100
Hole mobility (cm ² V ⁻¹ s ⁻¹)	2000	170	1.6	250
Shallow donor doping (cm ⁻³)	2×10^{19}	0	0	1×10^{16}
Shallow acceptor doping (cm ⁻³)	0	10^{15}	2.4×10^{17}	0
Total defect density (cm ⁻³)	10^{14}	10^{14}	10^{14}	10^{14}
Radiative recombination coefficient (cm ⁻³)	0	0	0	0
Series Resistance (Ω cm ²)	0	0	0	0
Shunt Resistance (Ω cm ²)	Infinite	Infinite	Infinite	Infinite
References	[21]	[21]	[21]	[21]

- Primary Input Parameters taken by SCAPS-1D and their default values.

Table S2: Primary Input parameters in SCAPS-1D and their default values

Parameter	Default value
General parameters	
Temperature (K)	300
Series Resistance	No
Shunt Resistance	No
Reflection	0%
Transmission	100%
Material specific parameters	
Radiative Recombination Coefficient (cm ³ /s)	0
Auger electron capture coefficient (cm ⁶ /s)	0
Auger hole capture coefficient (cm ⁶ /s)	0
Thickness (nm)	-
E _g (eV)	-
χ (eV)	-
Dielectric permittivity (ϵ_r)	-
DOS _{CB} (cm ⁻³)	-
DOS _{VB} (cm ⁻³)	-
Electron Thermal velocity (cm/sec)	-
Hole Thermal velocity (cm/sec)	-
Electron mobility (cm ² V ⁻¹ s ⁻¹)	-
Hole mobility (cm ² V ⁻¹ s ⁻¹)	-
Shallow donor doping (cm ⁻³)	-
Shallow acceptor doping (cm ⁻³)	-
Allow tunnelling	No
Effective mass of electrons	1
Effective mass of holes	1
Absorption model	'sqrt(hv-Eg) law (SCAPS traditional)'

Defect parameters

Defect Type	Neutral
capture cross section electrons (cm ²)	1.000E-15
capture cross section holes (cm ²)	1.000E-15
energetic distribution	Single
reference for defect energy level Et	Above Ev
energy level with respect to Reference (eV)	0.6
Characteristic energy (eV)	0.1
N _t total (cm ⁻³)	1.000E+14
Optical capture of electrons	Optional
Optical capture of holes	Optional

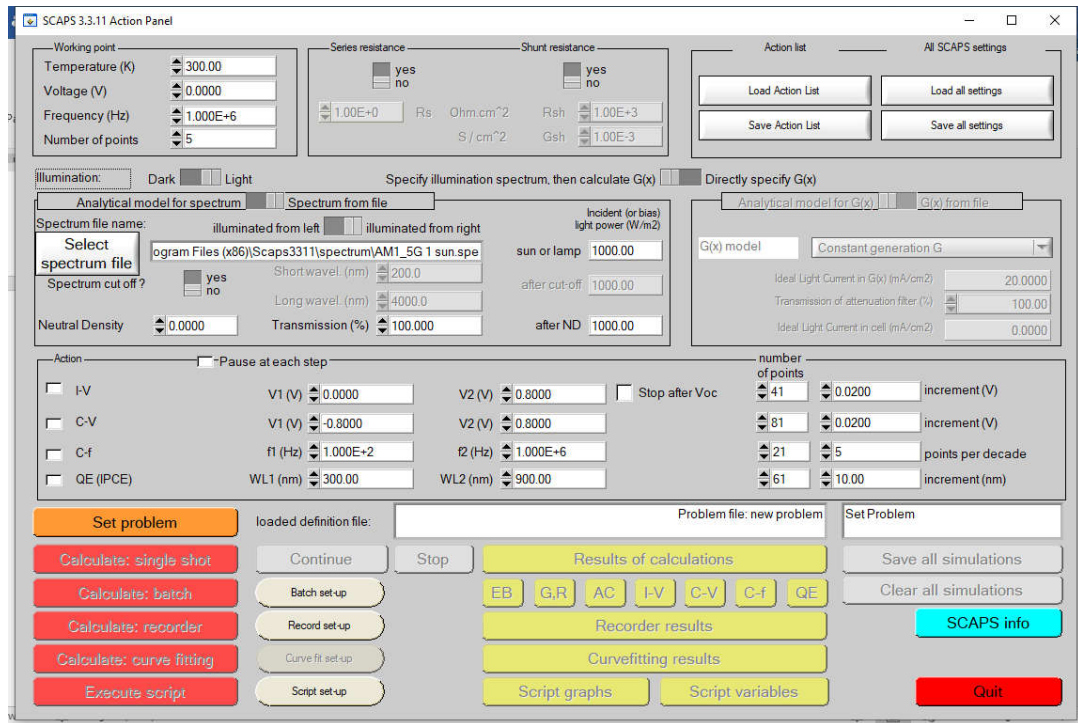


Figure S1: Screenshot of the Action Panel of SCAPS-1D, displaying the default general input parameters.

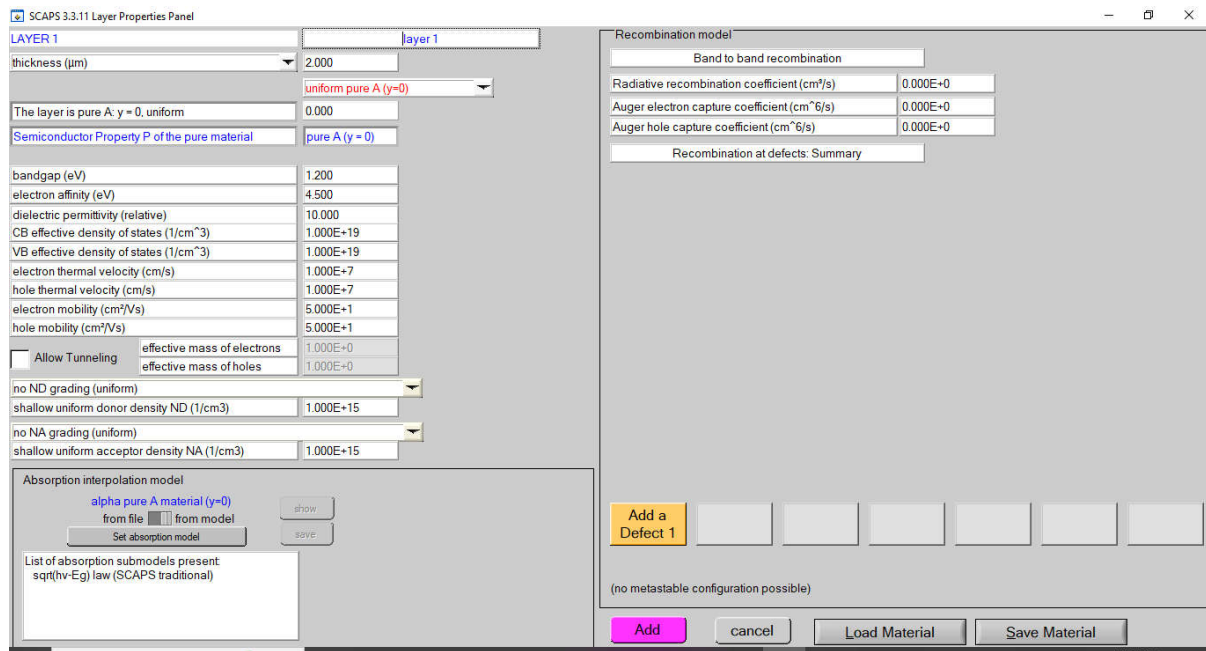


Figure S2: Screenshot of the Layer Properties Panel, displaying the default values of material specific input parameters.

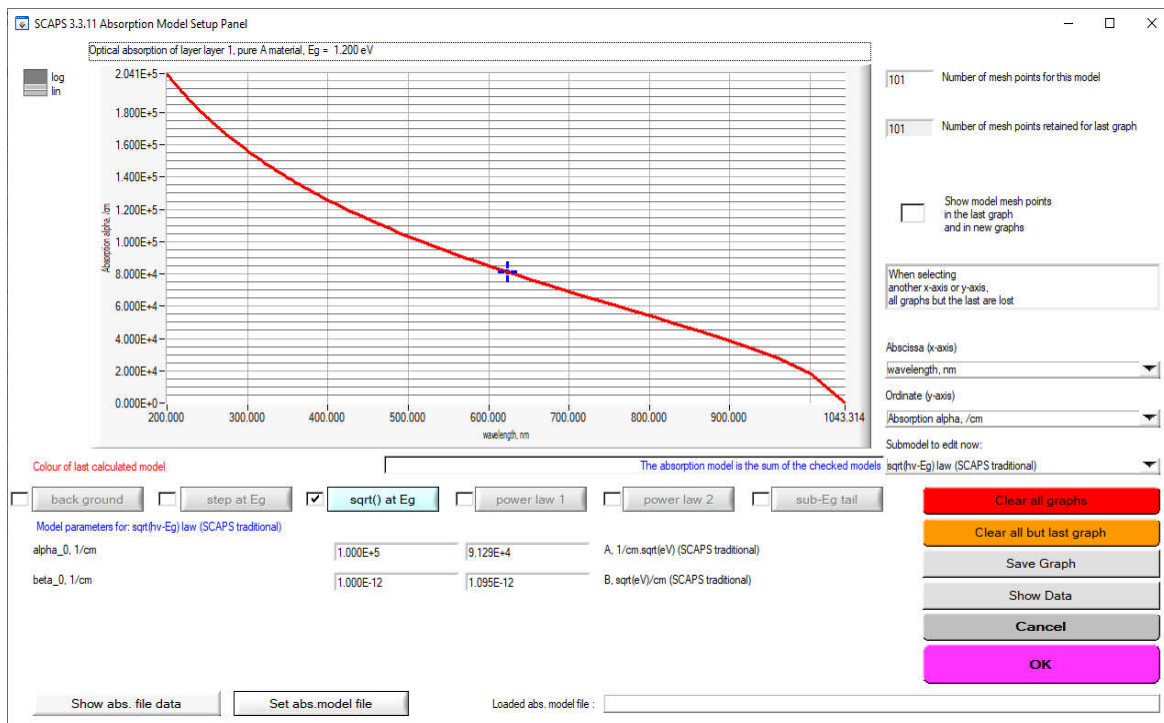


Figure S3: Screenshot of the Absorption Model Setup Panel, displaying the default absorption model in SCAPS-1D

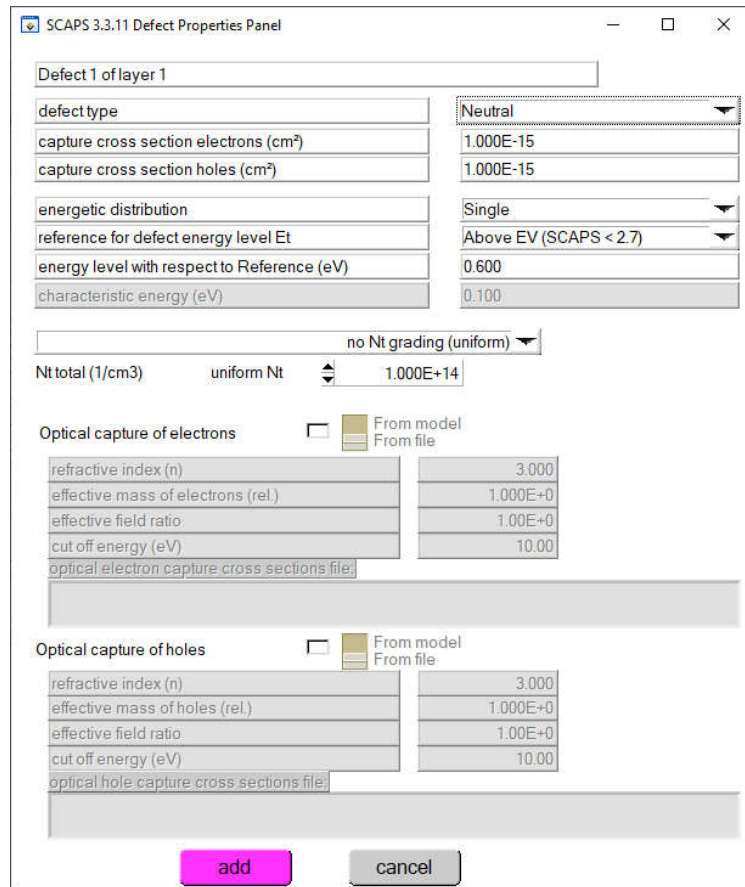


Figure S4: Defect Properties Panel in SCAPS-1D, displaying the default defect settings.

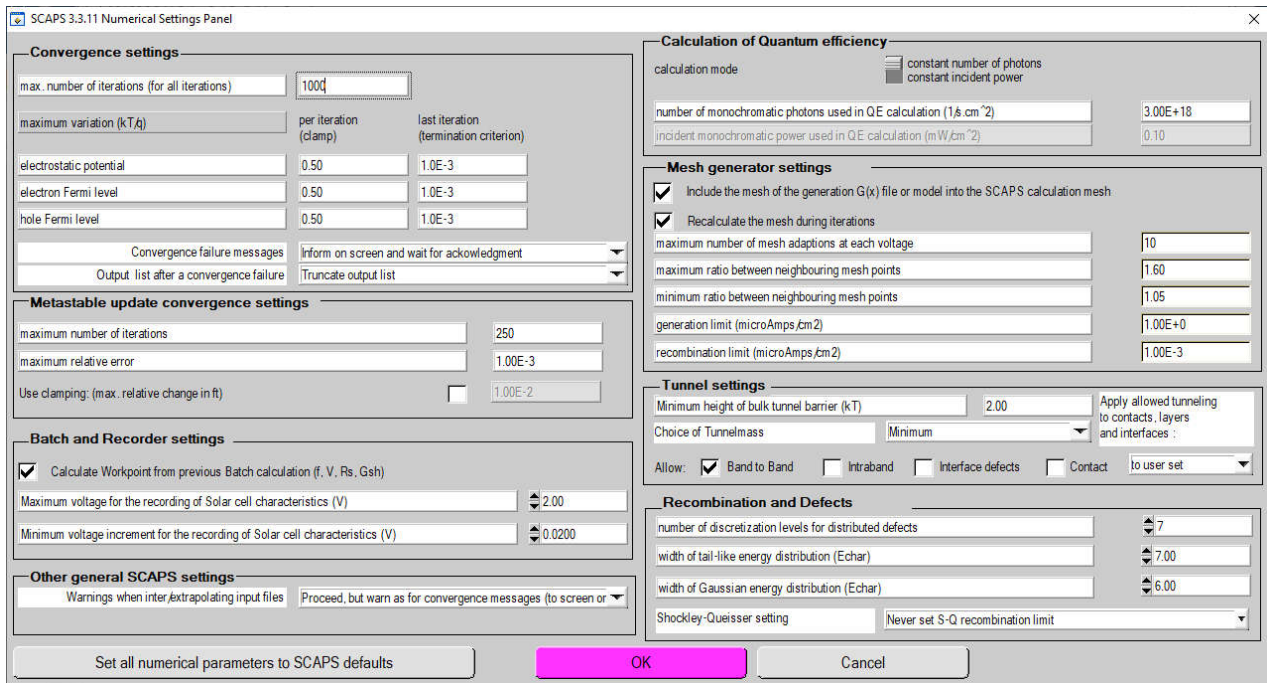


Figure S5: Numerical Settings Panel, displaying the default numerical settings used for SCAPS-1D simulations. Note that the default Shockley-Queisser setting is set as ‘Never set S-Q recombination limit’.

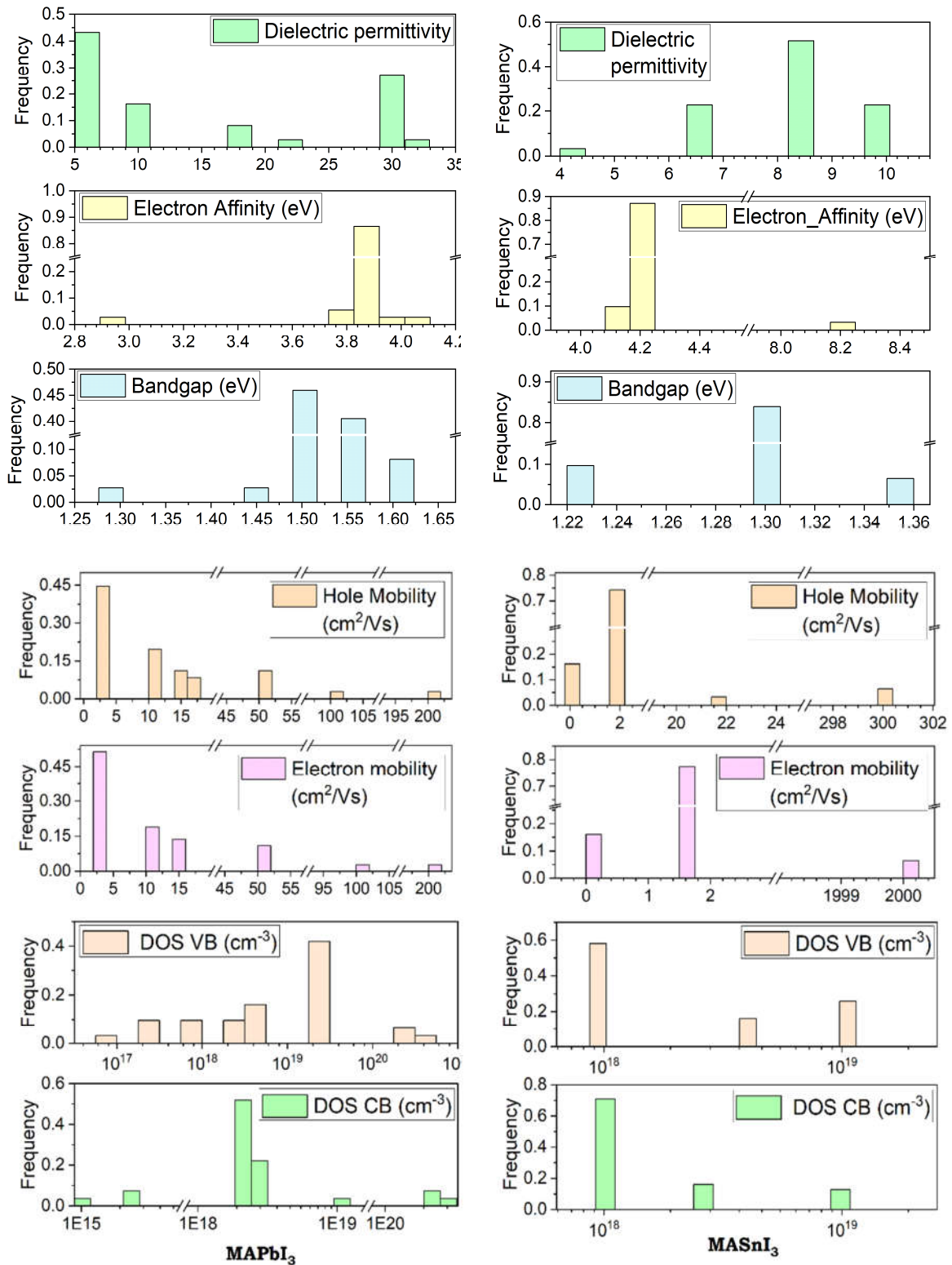


Figure S6: Variability in the values of the input parameters used for the simulations of MAPbI_3 and MASnI_3 -based perovskite solar cells using SCAPS-1D found in the survey.

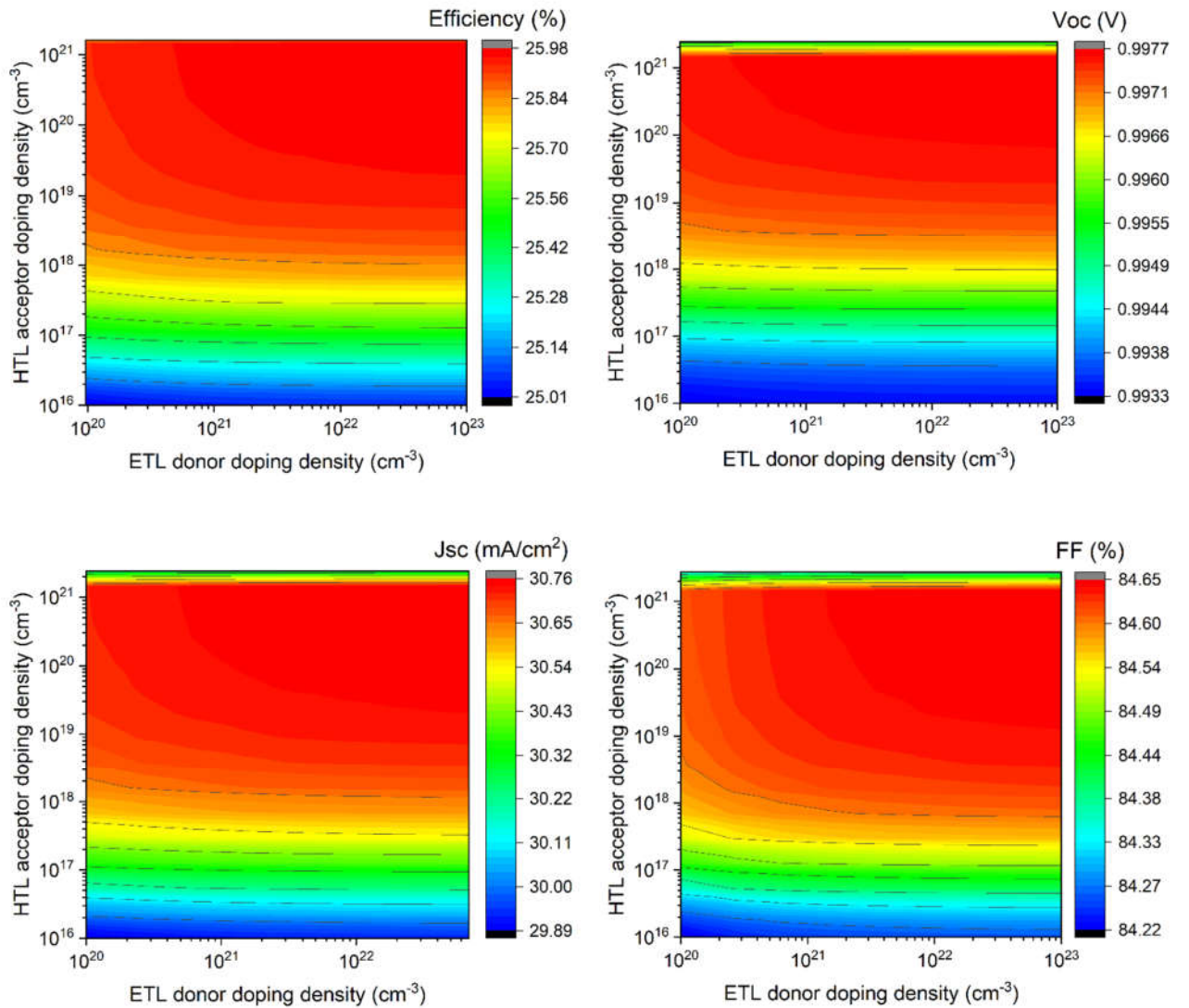


Figure S7: Dependence of device performance on the shallow doping concentrations for ETL and HTL for the device architecture described in the paper referenced as [21] with input parameters described in Table S1.

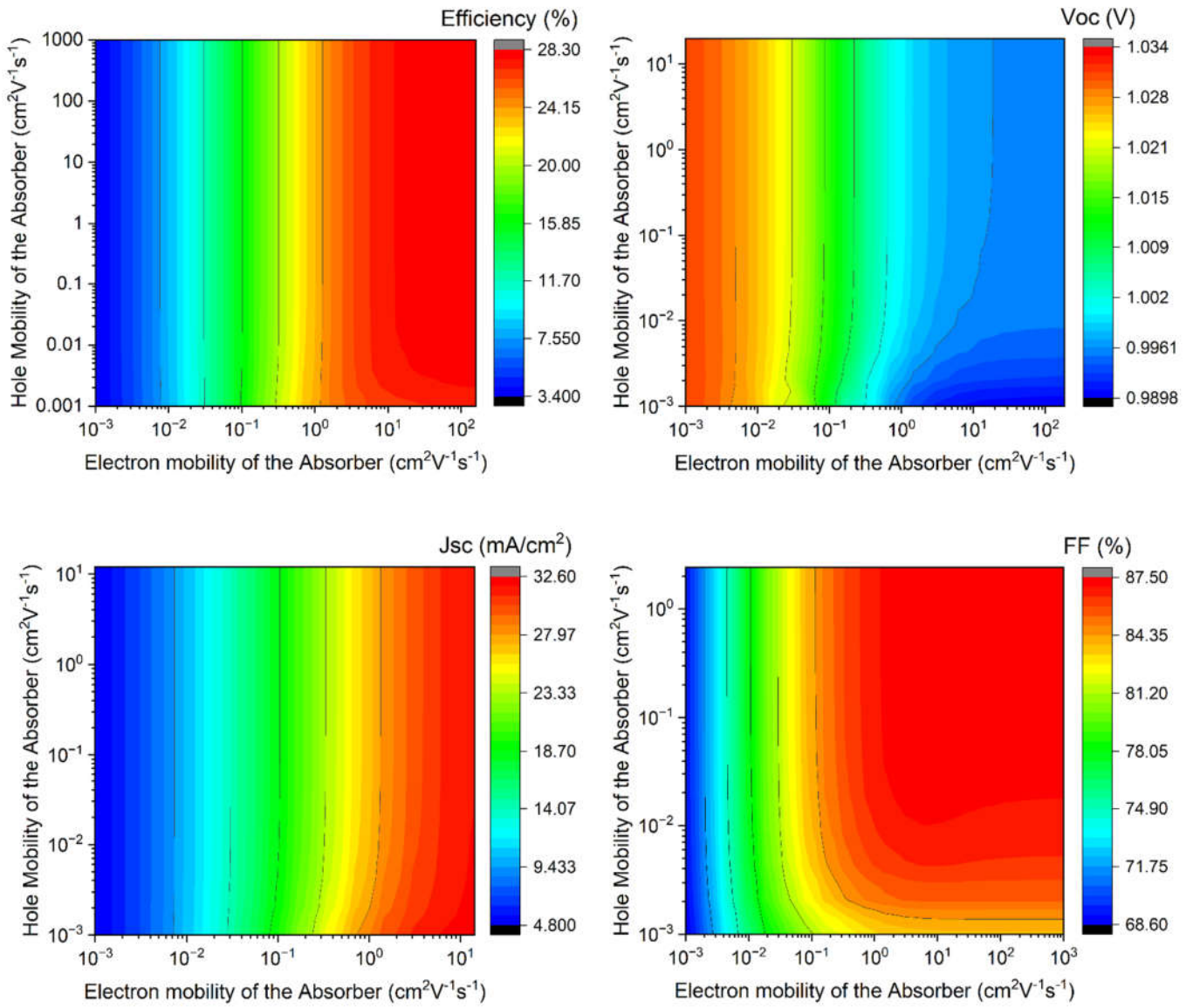


Figure S8: Dependence of device performance on the electron and hole mobilities of the absorber layer for the device architecture described in the paper referenced as [21] with input parameters described in Table S1.

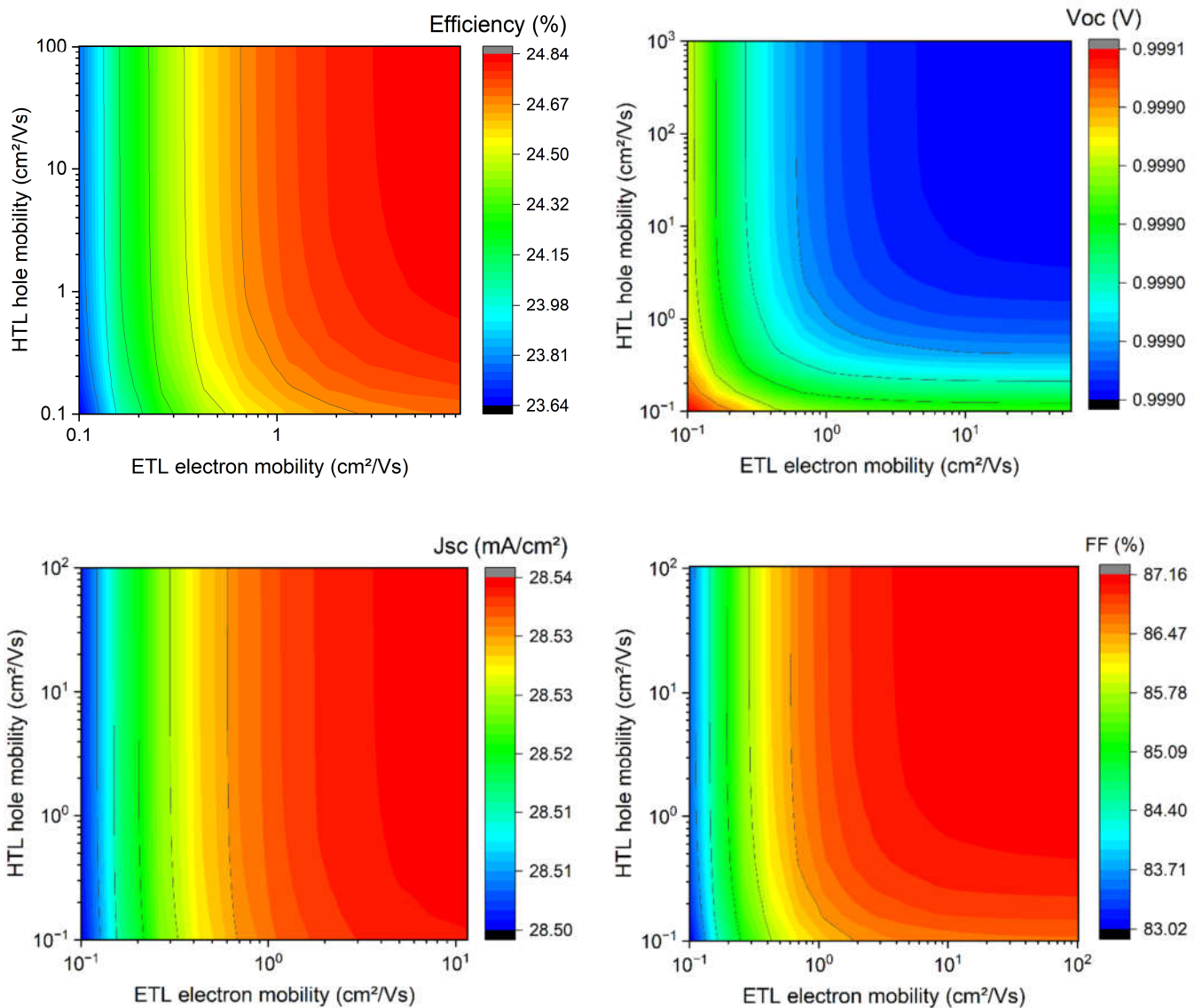


Figure S9: Dependence of device performance on the ETL electron mobility and HTL hole mobility for the device architecture described in the paper referenced as [21] with input parameters described in Table S1.

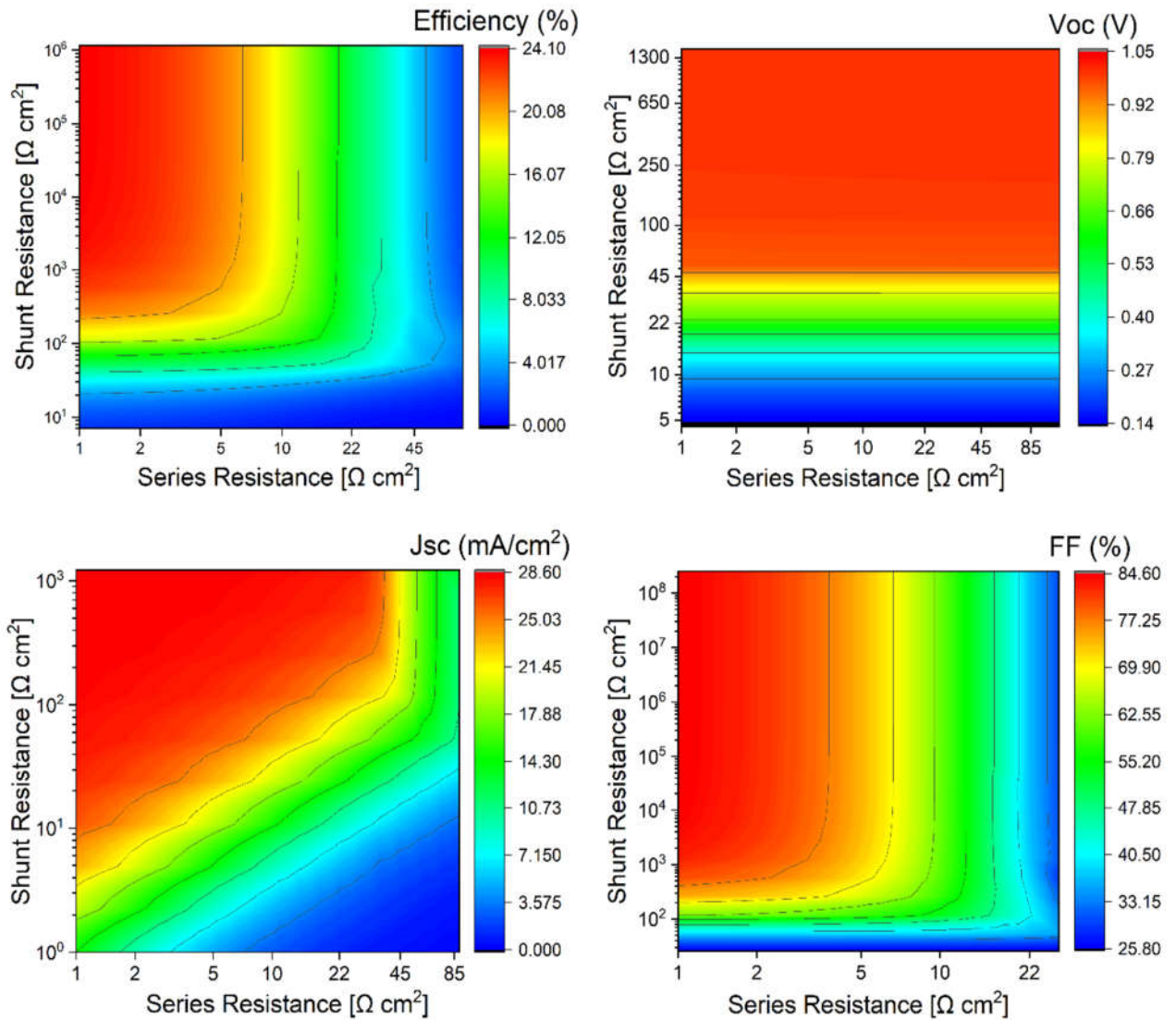


Figure S10: Dependence of device performance on external series and shunt resistance for the device architecture discussed in the paper referenced as [21] with input parameters described in Table S1.